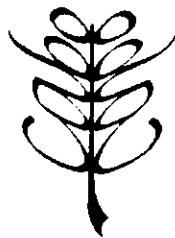


AGRISCATT
Quality analysis and data description of the DUTSCAT 1987 data.

B.A.M. Bouman
M.A.M. Vissers
D. Uenk

CABO report no. 135
1990



Centre for Agrobiological Research
P.O. Box 14, 6700 AA Wageningen, The Netherlands

Centre for Agrobiological Research (CABO)

P.O. Box 14,
6700 AA Wageningen
The Netherlands
Telefax: (+31)(0)8370-23110
Telex: 75209 cabo nl
Bitnet: pri@cabo.agro.nl

Bouman, B.A.M., M.A.M. Vissers and D. Uenk

AGRISCATT. Quality analysis and data description of the DUTSCAT 1987 data.
Centre for Agrobiological Research (CABO), Wageningen, The Netherlands, 48 pages

© Centre for Agrobiological Research (CABO), 1990

All rights reserved. No part of this publication may be reproduced, stored in a retrieval system, or transmitted, in any form or by any means, electronic, mechanical, photocopying, recording or otherwise, without the prior permission of CABO.

Contents

| | |
|-------------------------------|----|
| Abstract | 1 |
| Preface | 3 |
| List of tables and figures | 5 |
| 1 Introduction | 7 |
| 1.1 The Flevopolder test site | 7 |
| 1.2 DUTSCAT radar data | 7 |
| 2 General quality analysis | 9 |
| 2.1 Track plots | 9 |
| 2.2 Standard deviation. | 12 |
| 2.3 Final data selection. | 17 |
| 3 Qualitative description | 19 |
| 3.1 Angular behaviour. | 19 |
| 3.2 Crop type discrimination. | 23 |
| 3.3 Temporal behaviour. | 27 |
| 4 Summary and conclusions | 39 |
| References | 41 |

Abstract

A quality analysis and a visual data interpretation (graphs, figures) were carried out on the DUTSCAT radar data, collected over the Dutch test site in the Flevopolder in 1987 during the Agriscatt campaign. Data interpretation was related to crop type and crop growth of sugar beet, potato and winter wheat.

After rigorous quality analysis, the whole C-, X- and Ku2-band, all the measurements at 70° incidence angle and all field-average γ values with standard deviation > 3 dB were removed from the data set (unreliable data).

The relative position of the frequency bands was in accordance with general theory: γ L-band < γ S-band < γ Ku1-band. The field-average γ values were well clustered per crop type in all frequency bands, angles of incidence and at all sorties. For each crop type, the angular dependency of γ was smooth in all frequency bands: with mainly bare soil, γ decreased a little with increasing incidence angle, and with closed crop cover γ was more or less horizontal with incidence angle.

Crop types and fields of mainly bare soil could be discriminated in the different frequency bands. For mainly bare soil, a combination of the L- and the Ku1-band offered the best possibilities for soil-type discrimination ('beet-soil' from 'potato-soil' from 'wheat-soil' (70% crop cover)). For crop types, the best combination of frequency bands for discrimination was the L-band with the S-band.

The temporal curves of γ of the crop types were comparable in trend in all three frequency bands. For beet and potato, γ increased with crop growth until the midst of the growing season (beginning July). For wheat, no 'radar-growth' curves were recognized. The range in γ with the growth of the crops was generally not very large, i.e. in the order of 4-6 dB in all three frequency bands and for all crops (at 40° incidence angle). An exception was the L-band for potato in which the range was about 10 dB.

Preface

In 1987 the European Space Agency (ESA) and the Joint Research Centre (JRC) of the European Community initiated the Agriscatt 1987-1988 campaign. Airborne radar measurements were made of selected agricultural test sites in Europe through the growing season. These measurements included both multiband scatterometer data [DUTSCAT (1987, 1988), ERASME (1988)] and radar imagery in the X-band [SLAR (1987), VARAN-S (1987)], and in the C-band [IRIS (1987)]. Together with the radar measurements, groundtruth was collected on crops and bare soils. The main objective of the campaign was the preparation of future spaceborne SAR sensors and their use in land applications.

A Dutch team of ROVE (Radar Observation on VEgetation) participated in Agriscatt with a test site in Flevoland. The Centre for Agrobiological Research (CABO) collected the groundtruth on agricultural crops in 1987, and groundtruth on both crops and soil in 1988. In the framework of the National Remote Sensing Program (NRSP), the CABO embarked on a study to analyse the DUTSCAT radar data collected over the Flevopolder in relation to crop type and crop growth of sugar beet, potato and winter wheat (BCRS project AO-2.19). The purpose of this study was to compare the backscatter behaviour of agricultural crops in different frequency bands (1.2-17.3 GHz), and to draw preliminary conclusions on the use of multi-frequency radar observations for crop classification and growth monitoring. The analysis tools consisted of phenomenological data description, statistical correlation and principal component transformation [physical data analysis and modelling was undertaken at the Agricultural University of Wageningen, BCRS project AO-2.15]. This report, CABO report no. 135, and CABO report no. 136 presents the results of this study.

In 1987, all DUTSCAT data were unfortunately compressed during recording due to wrong attenuator settings. In an elaborative process, these data were decompressed through an especially designed decompression algorithm and became available for analysis only in April 1989. Also, during some sorties, data in some frequency bands, incidence angles or states of polarization were affected by instrument failure. During all recordings, a hardware failure resulted in a loss of some 30 dB in the X-band.

In 1988, data compression only occurred during the first two (of seven) sorties, while the X-band was not hampered by hardware failure. The difference in data quality between the 1987 and the 1988 data set led to separate data analysis at the CABO, and to the presentation of two reports. Report no. 135 largely focuses on quality analysis of the 1987 data set, and report no. 136 elaborates (the originally planned) data interpretation of the 1988 data set and gives the preliminary conclusions for use of these multi-band data in agriculture.

This project was carried out with the financial support of the Netherlands remote sensing board (BCRS), project AO-2.19.

List of tables and figures

Tables:

Table 1 Correction values on received power from corner responses, due to non-coherent adding in the DUTSCAT digital processor.

Table 2 General overview of the final DUTSCAT 87 dataset.

Figures:

Fig. 1 Location of the Dutch Agriscatt test site in South Flevoland

Fig. 2 The seven test parcels with the DUTSCAT flight line. The fields of ground truth collection are schematically indicated.

Fig. 3 Radar backscatter (sortie 2, HH 20° i.a.) along the flight track

Fig. 4 Radar backscatter (sortie 2, VV 20° i.a.) along the flight track

Fig. 5 Radar backscatter (sortie 5, HH 40° i.a.) along the flight track

Fig. 6 Radar backscatter (sortie 5, VV 40° i.a.) along the flight track

Fig. 7 Standard deviation (sortie 5, X-band, VV, 40° i.a.) versus radar backscatter

Fig. 8 Standard deviation (sortie 5, Ku2-band, VV, 40° i.a.) versus radar backscatter

Fig. 9 Frequency distribution of the standard deviation of the radar backscatter (L-band, sortie 1-6) in steps of 0.2 dB

Fig. 10 Frequency distribution of the standard deviation of the radar backscatter (S-band, sortie 1-6) in steps of 0.2 dB

Fig. 11 Frequency distribution of the standard deviation of the radar backscatter (C-band, sortie 1-6) in steps of 0.2 dB

Fig. 12 Frequency distribution of the standard deviation of the radar backscatter (X-band, sortie 1-6) in steps of 0.2 dB

Fig. 13 Frequency distribution of the standard deviation of the radar backscatter (Ku1-band, sortie 1-6) in steps of 0.2 dB

Fig. 14 Frequency distribution of the standard deviation of the radar backscatter (Ku2-band, sortie 1-6) in steps of 0.2 dB

Fig. 15 Radar backscatter of 'beet-soil', 'potato-soil' and 'wheat-soil' (sortie 1, L-band, VV) as a function of incidence angle

Fig. 16 Radar backscatter of beet, potato and wheat (sortie 4, L-band, VV) as a function of incidence angle

Fig. 17 Radar backscatter of 'beet-soil', 'potato-soil' and 'wheat-soil' (sortie 1, S-band, VV) as a function of incidence angle

Fig. 18 Radar backscatter of beet, potato and wheat (sortie 4, S-band, VV) as a function of incidence angle

Fig. 19 Radar backscatter of 'beet-soil', 'potato-soil' and 'wheat-soil' (sortie 1, Ku1-band, VV) as a function of incidence angle

Fig. 20 Radar backscatter of beet, potato and wheat (sortie 4, Ku1-band, VV) as a function of incidence angle

Fig. 21 Feature space plot (sortie 1, VV, 30° i.a.) of the S-band versus the L-band of 'beet-soil', 'potato-soil' and 'wheat-soil'

Fig. 22 Feature space plot (sortie 4 & 5, VV, 20° & 30° i.a.) of the S-band versus the L-band for potato, beet and wheat

Fig. 23 Feature space plot (sortie 1, VV, 30° i.a.) of the Ku1-band versus the L-band of 'beet-soil', 'potato-soil' and 'wheat-soil'

Fig. 24 Feature space plot (sortie 4 & 5, VV, 20° & 30° i.a.) of the Ku1-band versus the L-band for potato, beet and wheat

Fig. 25 Feature space plot (sortie 1, VV, 30° i.a.) of the Ku1-band versus the S-band of 'beet-soil', 'potato-soil' and 'wheat-soil'

Fig. 26 Feature space plot (sortie 4 & 5, VV, 20° & 30° i.a.) of the Ku1-band versus the S-band for potato, beet and wheat

Fig. 27 Radar backscatter of beet (L-, S-, Ku1-band, VV, 40° i.a.) in the course of the growing season

Fig. 28 Crop cover and dry biomass of beet in the course of the growing season, averaged for all fields

Fig. 29 Leaf Area Index (LAI) of beet in the course of the growing season, the numbers in the legend refer to the fieldnumbers of the crops

Fig. 30 Radar backscatter of potato (L-, S-, Ku1-band, VV, 40° i.a.) in the course of the growing season

Fig. 31 Crop cover and dry biomass of potato in the course of the growing season, averaged for all fields

Fig. 32 Leaf Area Index (LAI) of potato in the course of the growing season, the numbers in the legend refer to the fieldnumbers of the crops

Fig. 33 Radar backscatter of wheat (L-, S-, Ku1-band, VV, 40° i.a.) in the course of the growing season

Fig. 34 Crop cover and dry biomass of wheat in the course of the growing season, averaged for all fields

Fig. 35 Leaf Area Index (LAI) of wheat in the course of the growing season, the numbers in the legend refer to the fieldnumbers of the crops

Fig. 36 Average moisture content of the top soil (0-5 cm) of beet, potato and wheat in the course of the growing season

Fig. 37 Radar backscatter of the main croptypes (sortie 2, L-, S-, Ku1-band, VV, 20° i.a.)

Fig. 38 Radar backscatter of the main croptypes (sortie 2, L-, S-, Ku1-band, VV, 40° i.a.)

Fig. 39 Radar backscatter of the main croptypes (sortie 5, L-, S-, Ku1-band, VV, 20° i.a.)

Fig. 40 Radar backscatter of the main croptypes (sortie 5, L-, S-, Ku1-band, VV, 40° i.a.)

1 Introduction

This report presents a quality analysis and a visual data interpretation (graphs, figures) of the DUTSCAT (Delft University of Technology SCATterometer) data collected over the Flevopolder in 1987 during the Agriscatt campaign. Data interpretation was related to crop type and crop growth of sugar beet, potato and winter wheat. The purpose of this study was to compare the backscatter behaviour of agricultural crops in different frequency bands (1.2-17.3 GHz), and to draw preliminary conclusions for crop classification and growth monitoring. Because of the problems encountered during DUTSCAT data recording in 1987 (see Preface), the analysis in this report focuses on data quality assessment (§ 2) and on a qualitative data description only (§ 3).

Overviews of the Agriscatt campaign and its objectives in general are given by Attema (1989) and by Hoekman (1990).

1.1 The Flevopolder test site

The test site was located in Southern Flevoland and comprised seven rectangular shaped agricultural parcels of about 80 ha. These parcels were subdivided into fields by the farmers to grow several crop types and varieties. Figure 1 gives the location of the test site in Southern Flevoland, and figure 2 illustrates the seven test parcels with the flight line of the (side-looking) DUTSCAT. All fields in the seven test parcels were measured by DUTSCAT.

During the DUTSCAT overpasses, ground truth was collected on three fields of sugar beet, potato and winter wheat. The ground truth comprised, amongst others: top soil moisture content (stratified in the layer of 0-5 cm), crop cover, crop height, fresh and dry canopy biomass and LAI. Visual observations were made of phenological development stage and any anomalies like disease infection or weed cover.

More details on the test site, and on the collected ground truth and measurement accuracy are given by Stolp et al. (1988).

1.2 DUTSCAT radar data

DUTSCAT was operated in six frequency bands: L- (1.2 GHz), S- (3.2 GHz), C- (5.3 GHz), X- (9.7 GHz), Ku1 (13.7 GHz) and Ku2 (17.3 GHz). The radar backscattering was measured six times in the growing season at vertical (VV) and horizontal (HH) co-polarization: May 18, June 1, June 15, July 6, July 31 and September 8 (numbered sortie 1-6 from here on). The incidence angles were 20°, 30°, 40°, 50° and 70°. At each angle of incidence, state of polarization and frequency, DUTSCAT was externally calibrated on corner reflectors for each sortie by the Technical University of Delft (TUD).

All DUTSCAT data in 1987 became compressed during recording due to wrong attenuator settings. Decompression of the data was carried out through an especially designed decompression algorithm at the TUD. Furthermore, a hardware failure during recording resulted in a loss of about 30 dB in the X-band. Therefore, this band could not be externally calibrated and was excluded for further analysis in this study. Technical details on the DUTSCAT, and on data decompression, processing and calibration are given by Snoeij and Swart (1987, 1988). A technical quality analysis of the DUTSCAT 1987 data was performed at ESA/EARTHNET (James, 1989).

The Physics and Electronics Laboratory TNO computed the average radar backscatter in γ (radar cross section per unit projected area), and the standard deviation, for all agricultural fields in the seven test parcels. Also, radar data of very low quality were already discarded (P. Luik, 1990).



Fig. 1 Location of the Dutch Agriscatt test site in South Flevoland

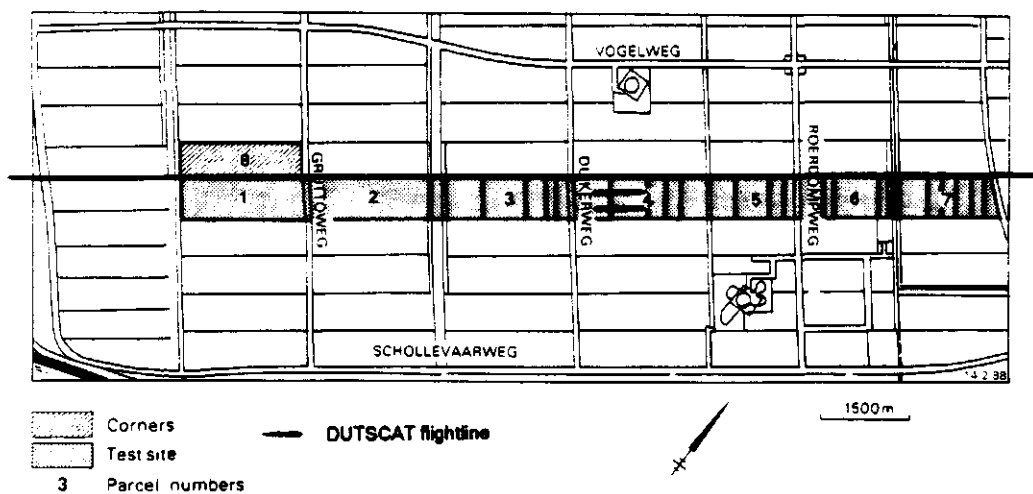


Fig. 2 The seven test parcels with the DUTSCAT flight line. The fields of ground truth collection are schematically indicated.

2 General quality analysis

2.1 Track plots

The first step was the analyses of 60 so called track plots. A track plot shows the radar backscatter of all fields along the flight track in all frequencies at one state of polarization and at one angle of incidence, for one sortie. In these plots the data in the X-band are excluded because they are not calibrated and their relative position has no meaning. Some examples of these plots are given in figures 3 to 6.

From this analysis, the following generalizations are derived:

- The relative position of the L-, S- and Ku-bands (together) looks good. As general theory predicts a higher frequency gives a higher radar backscatter. Deviations from this pattern occur only for some individual fields. In comparison with the L- and the Ku-bands, the dynamic range of the S-band is relatively low.
- The relative positions of both Ku-bands are not in accordance with general theory. They mutually alternate with different angles of incidence and states of polarization. The Ku1-band may either be higher, lower or on the same level as the Ku2-band. The patterns of both bands, however, are nearly identical; the bands are highly correlated.
- The relative position of the C-band is also in doubt because, like the Ku-bands, it is fluctuating (different relative positions with different incidence angles and states of polarization). The backscatter in the C-band appears correlated with that in the Ku-bands.
- In the frequency bands of the last three sorties the relative position of a (field average) γ value corresponds with the crop type on the field.

The track plots of the decompressed data look better than those of the original (compressed) data: the dynamic range in the various frequency bands has improved, and the relative position of the bands is also better. However, there still appear some 'suspicious' data in this set which regard individual fields in specific tracks as well as whole tracks.

CABO

Sortie 2; HH polarization; 20° incidence angle

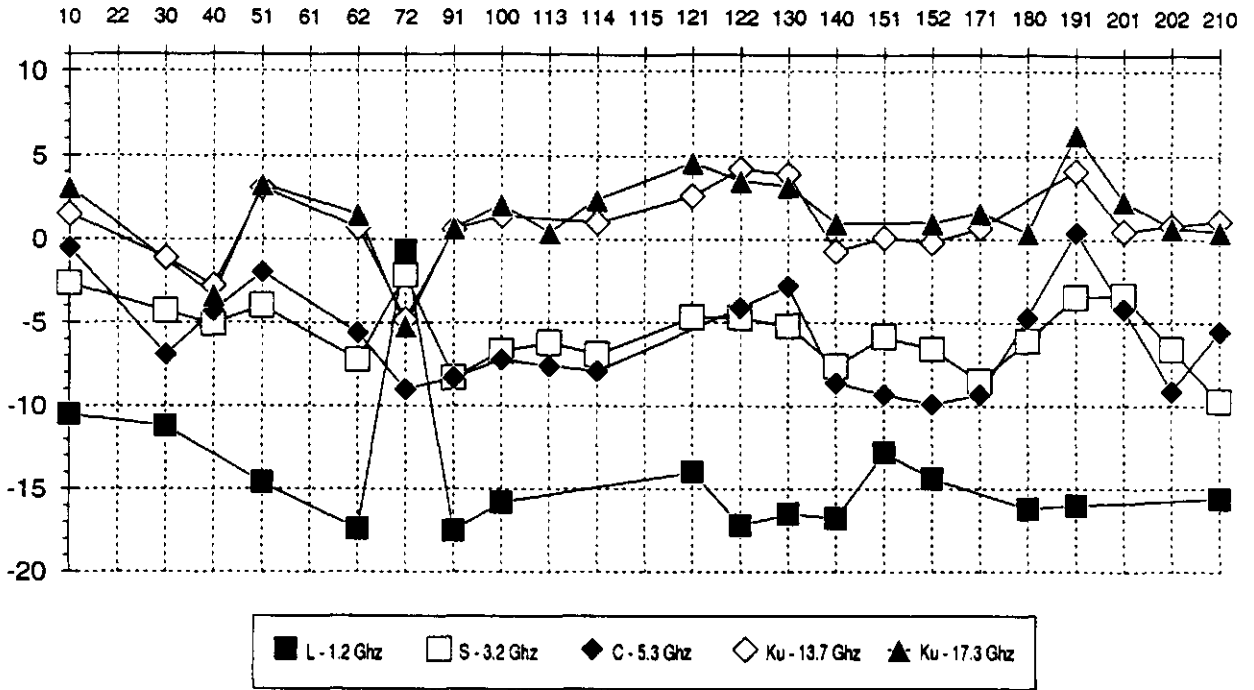


Fig. 3 Radar backscatter (sortie 2, HH 20° i.a.) along the flight track

CABO

Sortie 2; VV polarization; 20° incidence angle

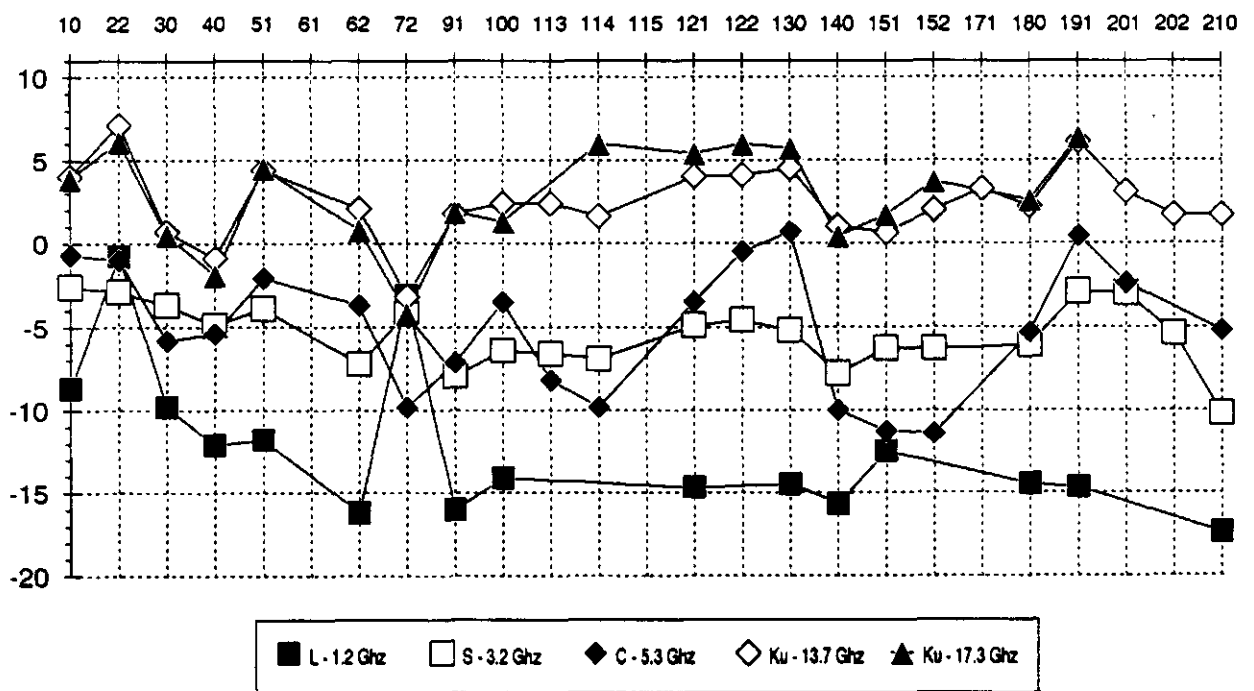


Fig. 4 Radar backscatter (sortie 2, VV 20° i.a.) along the flight track

CABO

Sortie 5; HH polarization; 40° incidence angle

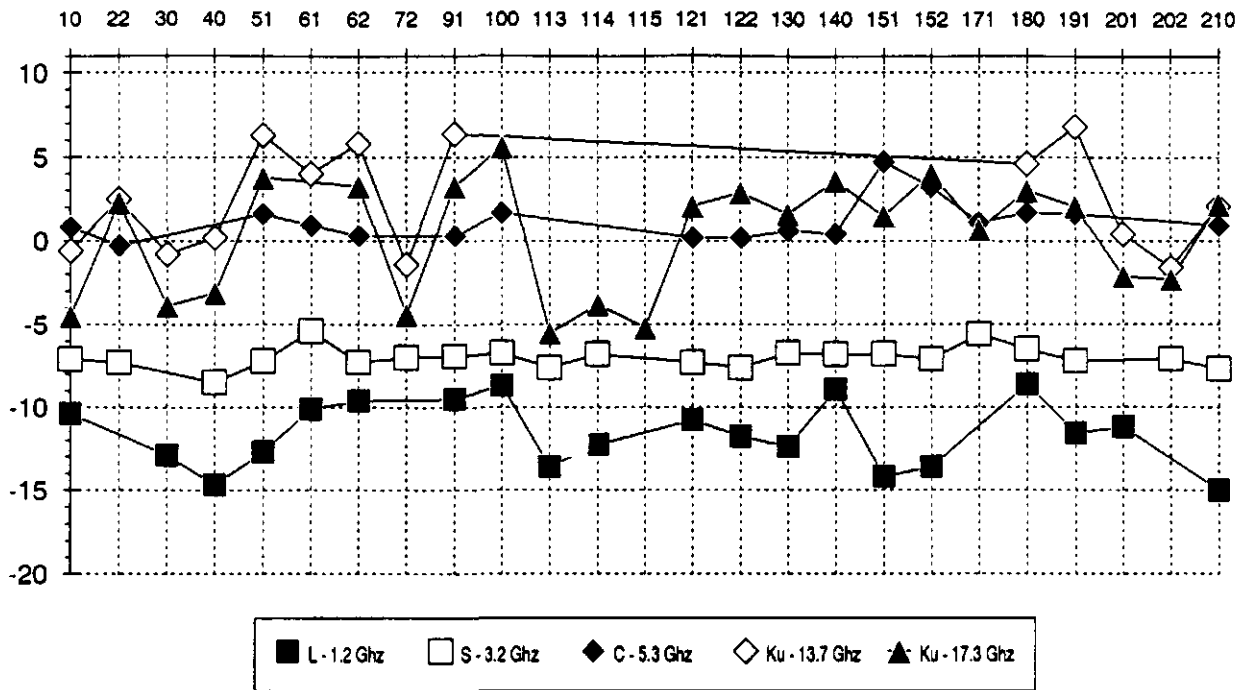


Fig. 5 Radar backscatter (sortie 5, HH 40° i.a.) along the flight track

CABO

Sortie 5; VV polarization; 40° incidence angle

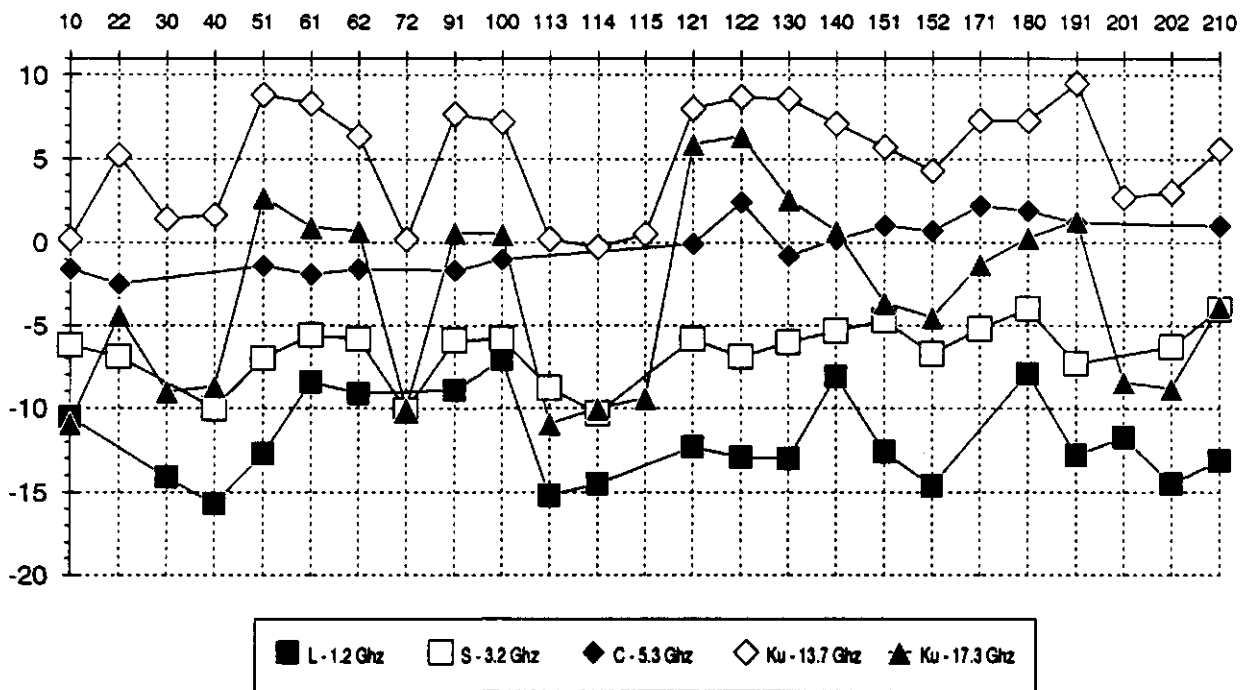


Fig. 6 Radar backscatter (sortie 5, VV 40° i.a.) along the flight track

2.2 Standard deviation.

Because of the non-linearity of the decompression algorithm (applied at the TUD), not all the data are corrected with the same 'reliability'. The higher the radar backscatter of a field, the more saturated the response was during recording and the more difficult it is to decompress the data. Therefore, it is to be expected that a field with a high return will have an average, decompressed γ value which is less 'reliable' than that of a field with a low return. Furthermore, if a complete band was too much saturated during recording, the decompression may lead to erroneous results for the whole band. Suspicious (unreliable) data can thus appear as single γ values in frequency bands which are generally well decompressed, or as whole frequency bands that were too saturated for reliable decompression. Part of such data were already removed through a selection procedure at the FEL-TNO, but a part still remains in the delivered data set (previous paragraph).

A way of recognizing these suspicious data is through their relation with other data and their standard deviation. In theory, the standard deviation of field-average backscatter values should be centred around 1 dB (Hoekman, pers. comm.). If the radar data were saturated during recording, the standard deviation of the field averages increases with the decompression. This is illustrated in figures 7-8 where the standard deviation is plotted against the field average γ for the decompressed Ku2-band and for the X-band (which was not saturated during recording). In the X-band the standard deviation is indeed nicely centred around 1 dB, regardless of the value of the field-average γ . In the Ku2-band, the same is true until a certain threshold of γ is reached. After this threshold, increasing values of γ are associated with increasing standard deviations. These suspicious data belong to fields with highly reflective (in the microwave region) crops, h.c. beet and potato. Therefore, the quality of the decompressed radar data is related to the type of the crop on the field.

To evaluate the performance of a whole frequency band, the frequency distribution of the standard deviation is investigated, figures 9-14. Again, the unsaturated X-band shows a distribution close around the theoretical 1 dB at all sorties but the sixth (?). The distribution for the L-, S- and Ku1-band appears also reasonably centred around 1 dB, but with more standard deviations in the classes > 2 dB. These deviations are related to a) recordings in the 70° incidence angle, and b) individual fields with a high radar backscatter. At 70° incidence angle the accuracy of measuring an individual field in the low frequency bands without contributions (noise) from surrounding fields is relatively low. This noise adds to the standard deviation of the field-average γ . The frequency distribution for the C- and Ku2-band deviates largely from that of the other bands. The standard deviation is irregularly spread over all the classes with a high occurrence in the class > 4 dB. This distribution is independent of the state of polarization and the angle of incidence.

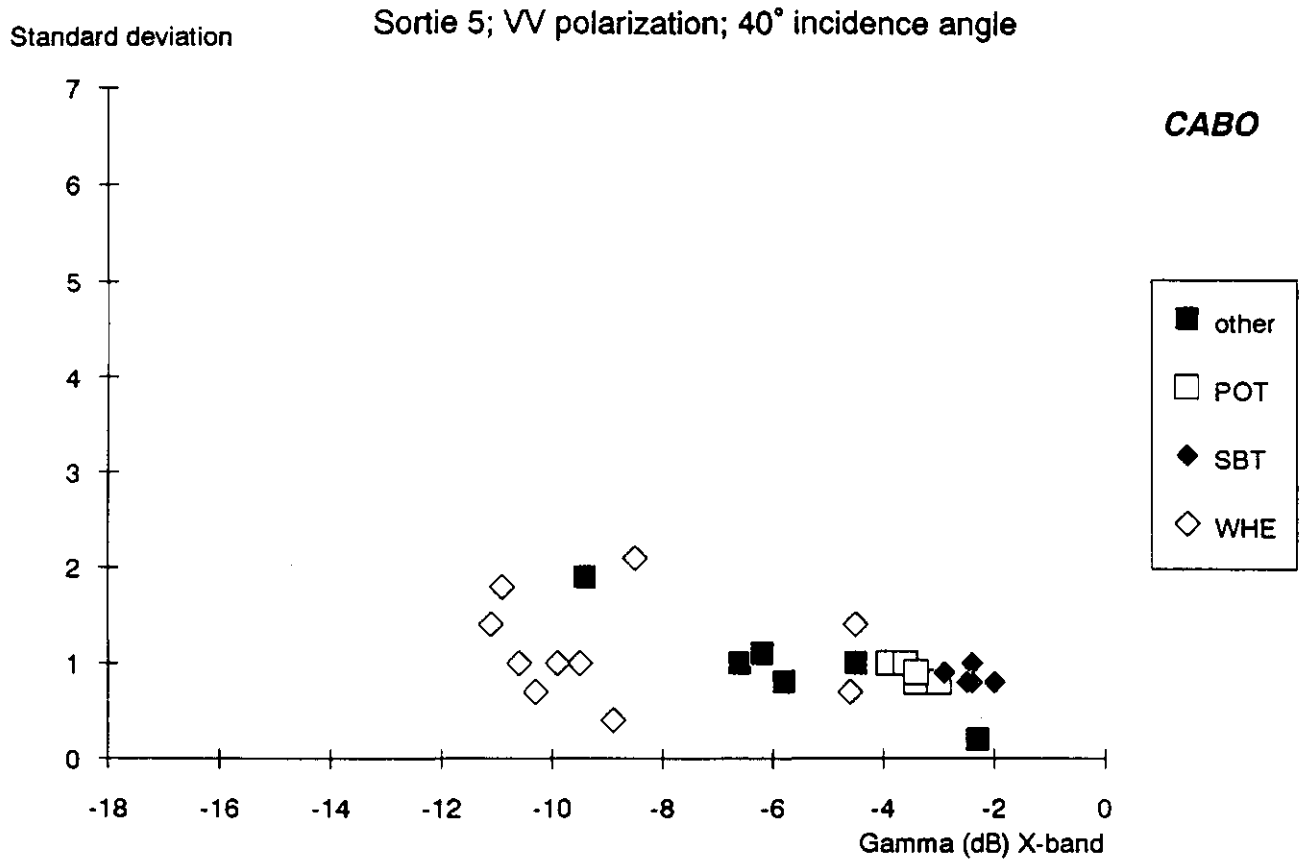


Fig. 7 Standard deviation (sortie 5, X-band, VV, 40° i.a.) versus radar backscatter

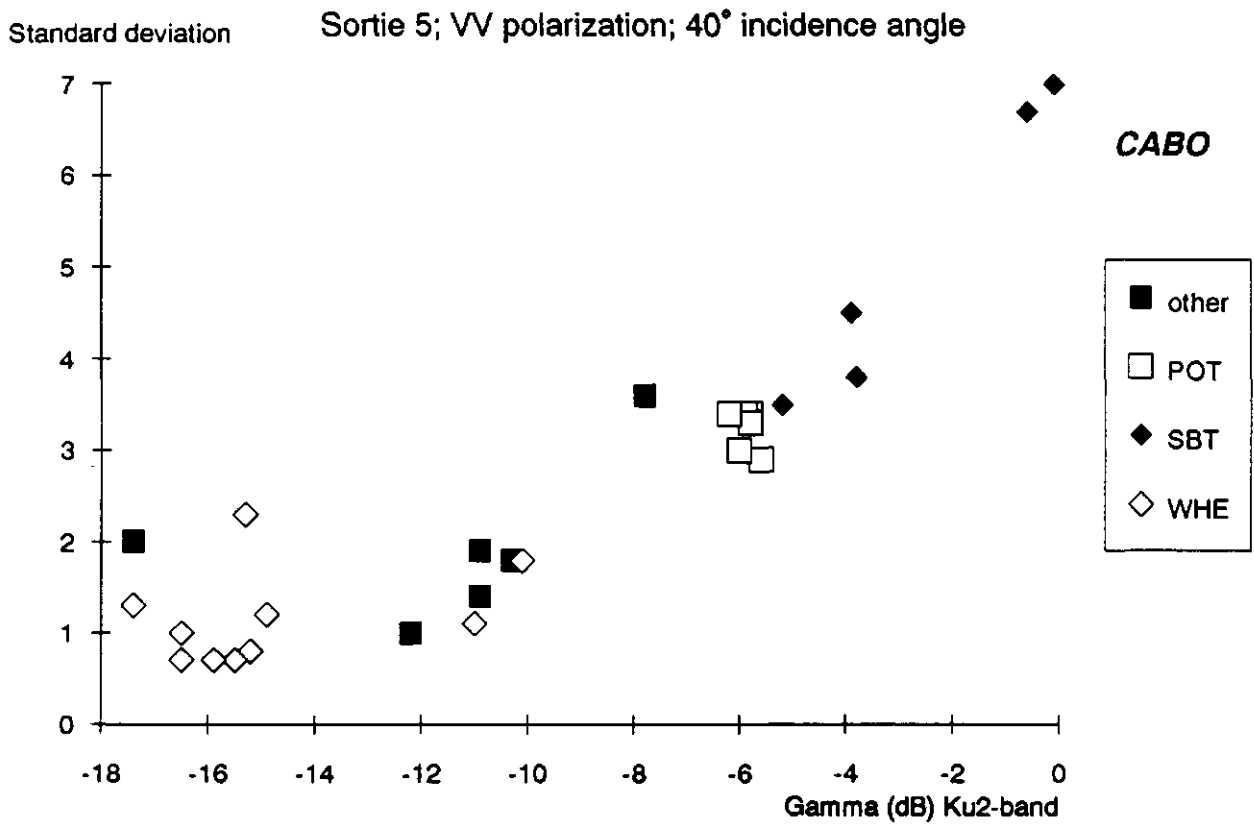


Fig. 8 Standard deviation (sortie 5, Ku2-band, VV, 40° i.a.) versus radar backscatter

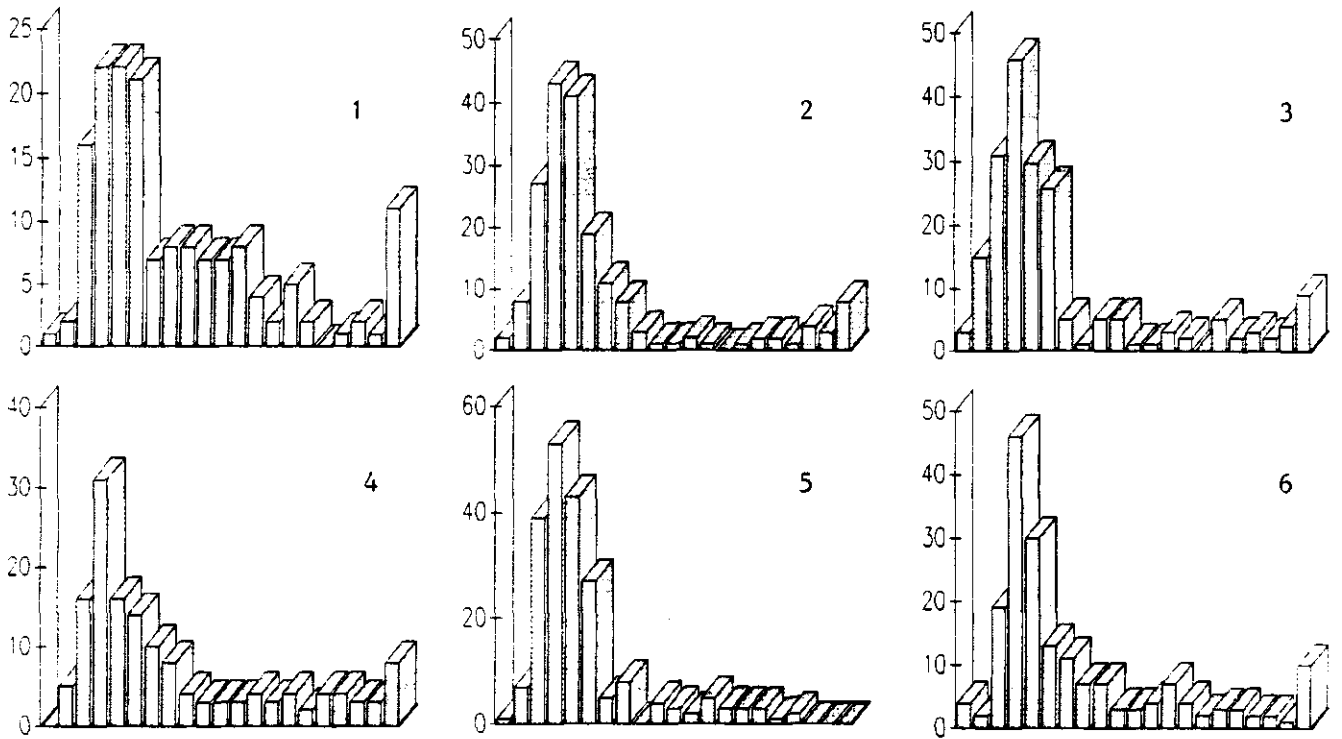


Fig. 9 Frequency distribution of the standard deviation of the radar backscatter (L-band, sortie 1-6) in steps of 0.2 dB

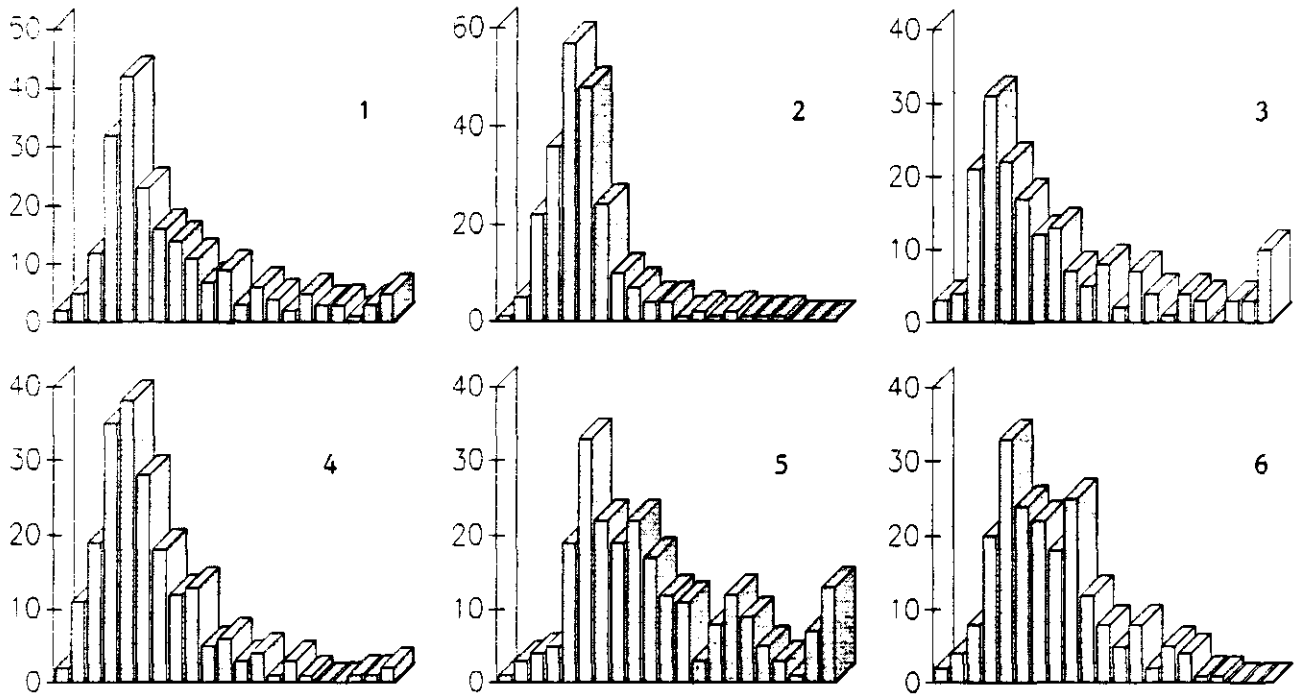


Fig. 10 Frequency distribution of the standard deviation of the radar backscatter (S-band, sortie 1-6) in steps of 0.2 dB

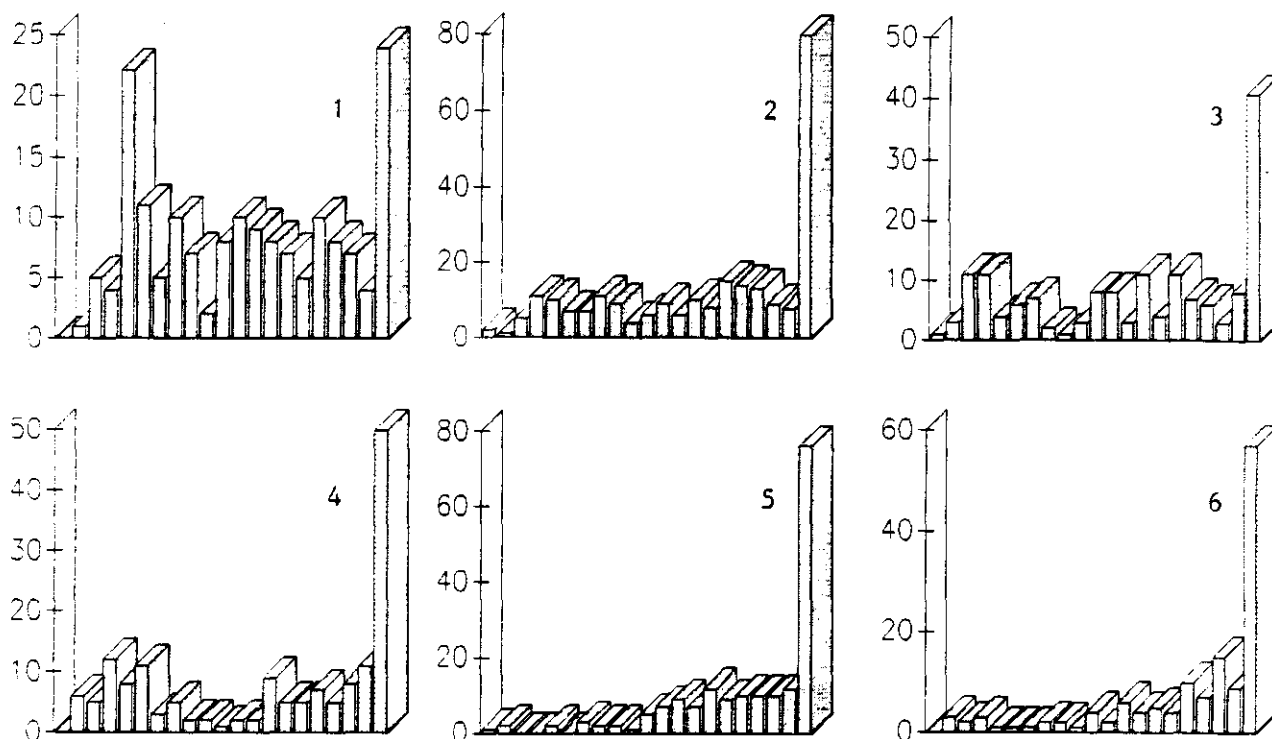


Fig. 11 Frequency distribution of the standard deviation of the radar backscatter (C-band, sortie 1-6) in steps of 0.2 dB

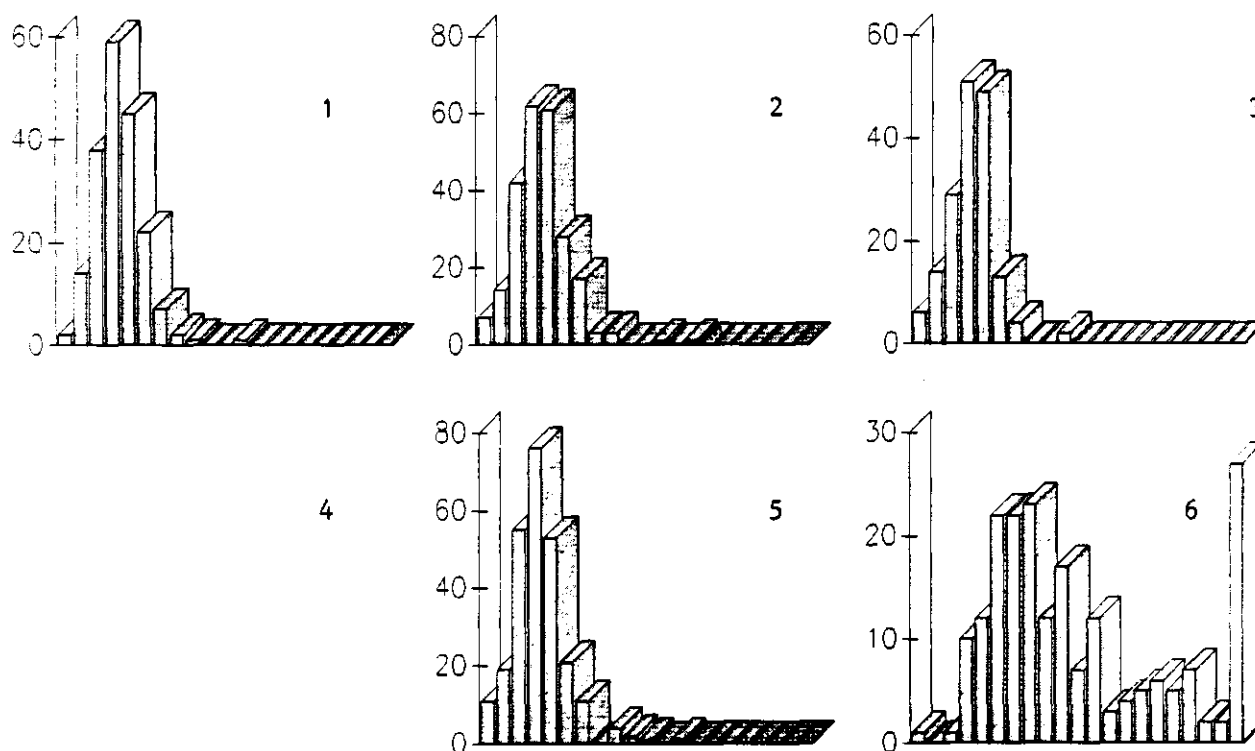


Fig. 12 Frequency distribution of the standard deviation of the radar backscatter (X-band, sortie 1-6) in steps of 0.2 dB

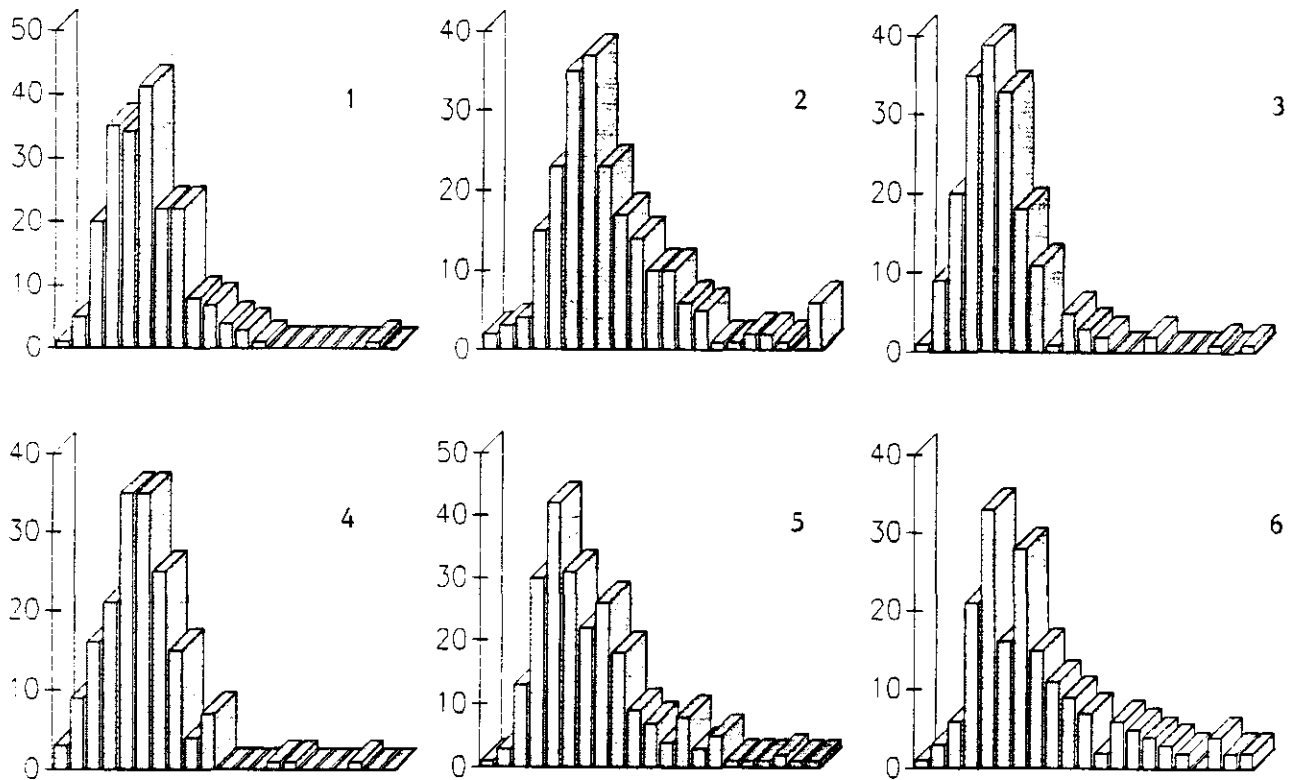


Fig. 13 Frequency distribution of the standard deviation of the radar backscatter (Ku1-band, sortie 1-6) in steps of 0.2 dB

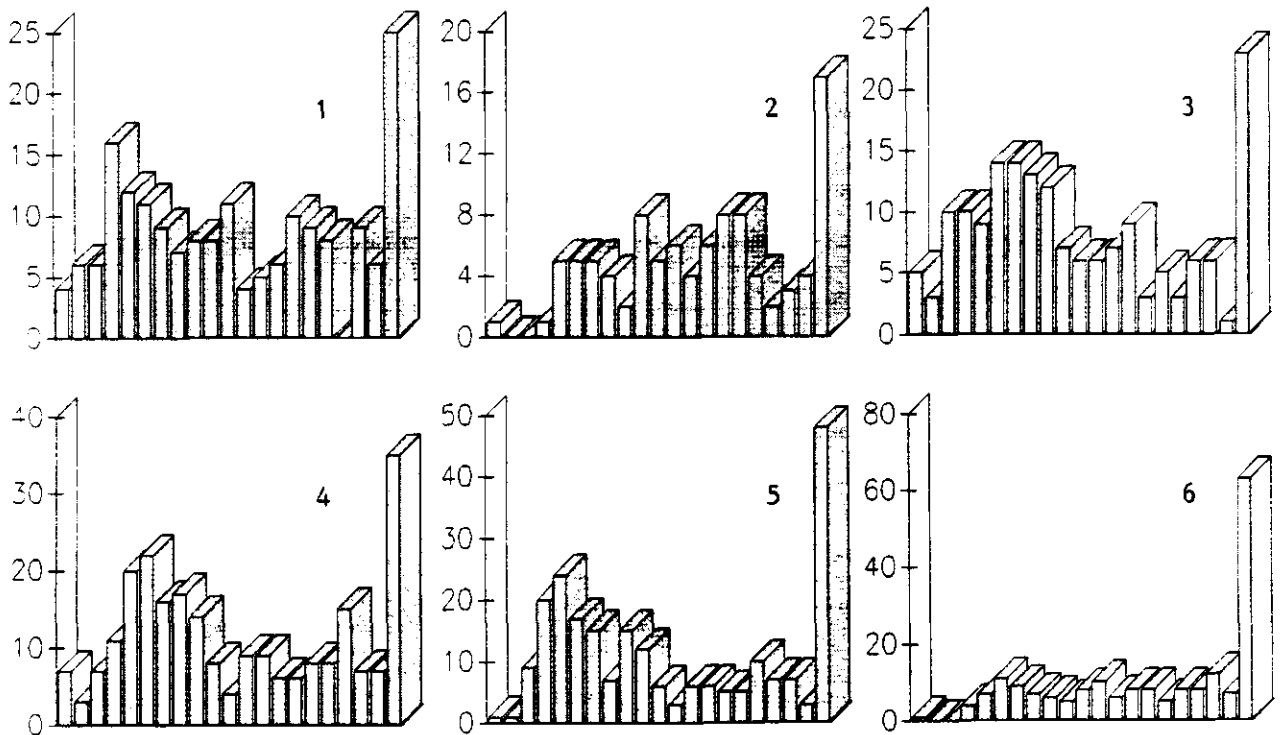


Fig. 14 Frequency distribution of the standard deviation of the radar backscatter (Ku2-band, sortie 1-6) in steps of 0.2 dB

2.3 Final data selection.

The combination of the analyses in the previous paragraphs leads to a rigorous removal of still suspicious data in the delivered set:

- 1) individual fields with a standard deviation of > 3 dB,
- 2) all measurements at 70° incidence angle (most of these measurements are also excluded on the basis of the first criterion),
- 3) the whole C- and Ku2-band (fluctuating relative positions in the track plots combined with the deviating distribution of the standard deviations; the loss of the Ku2-band is somewhat compensated for by the high correlation with the Ku1-band).

The data set that is left (at the CABO) for agronomic interpretation therefore consists of calibrated γ values in:

- L-, S- and Ku1-band,
 - 20° , 30° , 40° and 50° incidence angle,
 - VV and HH polarization,
 - (with standard deviations of < 3 dB).
- (The uncalibrated X-band data will be used for comparison only)

In July 1989, some last correction values had to be applied on the data set delivered in April, table 1. These were corrections for the non-coherent integration of the corner responses which had been forgotten during calibration and decompression at the TUD. These (additive) correction values however, do not affect the results of the quality analyses presented here.

Table 1 Correction values on received power from corner responses, due to non-coherent adding in the DUTSCAT digital processor.

| DUTSCAT frequency (GHz) | 1.2 | 3.2 | 5.3 | 9.7 | 13.7 | 17.3 |
|----------------------------|-----|-----|-----|-----|------|------|
| REC. POWER CORRECTION (dB) | 0.1 | 0.7 | 1.7 | 4.1 | 5.5 | 6.5 |

An overview of the final DUTSCAT 87 radar data set at the CABO, after calibration, decompression, correction and selection is given in table 2.

Table 2 General overview of the final DUTSCAT 87 dataset.

| | | L-band ; HH | | | | L-band ; VV | | | |
|-----|-------|---------------|-------|----|-------|---------------|------|----|--|
| SRT | MIN | MEAN | MAX | N | MIN | MEAN | MAX | N | |
| 1 | -23.3 | -15.9 | -7.2 | 49 | -18.5 | -13.4 | -8.1 | 51 | |
| 2 | -23.4 | -17.1 | -10.6 | 66 | -19.8 | -15.2 | -8.8 | 69 | |
| 3 | -21.4 | -14.6 | -10.5 | 67 | -19.0 | -13.1 | -9.3 | 67 | |
| 4 | -15.5 | -12.4 | -9.4 | 49 | -18.7 | -11.7 | -6.9 | 59 | |
| 5 | -15.1 | -11.1 | -6.2 | 70 | -16.1 | -11.2 | -5.1 | 75 | |
| 6 | -19.2 | -10.4 | -2.3 | 65 | -17.4 | -10.1 | -3.5 | 70 | |
| | | S-band ; HH | | | | S-band ; VV | | | |
| SRT | MIN | MEAN | MAX | N | MIN | MEAN | MAX | N | |
| 1 | -19.1 | -8.5 | -2.3 | 69 | -11.6 | -7.7 | 0.0 | 64 | |
| 2 | -14.0 | -9.0 | -3.4 | 84 | -12.9 | -8.5 | -3.3 | 87 | |
| 3 | -15.4 | -10.5 | -5.0 | 64 | -15.2 | -9.3 | -4.1 | 76 | |
| 4 | -9.7 | -6.7 | -2.0 | 67 | -13.5 | -7.6 | -2.6 | 81 | |
| 5 | -9.7 | -7.1 | -2.2 | 73 | -11.3 | -6.9 | -1.8 | 72 | |
| 6 | -12.7 | -7.6 | -3.5 | 68 | -10.9 | -7.1 | -3.6 | 78 | |
| | | X-band ; HH | | | | X-band ; VV | | | |
| SRT | MIN | MEAN | MAX | N | MIN | MEAN | MAX | N | |
| 1 | -4.6 | 1.1 | 4.9 | 62 | -3.1 | 1.3 | 5.1 | 62 | |
| 2 | -6.8 | -2.9 | 1.3 | 83 | -5.2 | -1.7 | 2.2 | 79 | |
| 3 | -4.7 | 0.1 | 4.6 | 84 | -2.1 | 1.6 | 6.6 | 78 | |
| 4 | | | | 0 | | | | 0 | |
| 5 | -9.1 | -3.8 | 3.0 | 83 | -11.5 | -4.2 | 3.0 | 87 | |
| 6 | -10.3 | -5.6 | -0.9 | 49 | -8.3 | -4.7 | -0.9 | 61 | |
| | | Ku1-band ; HH | | | | Ku1-band ; VV | | | |
| SRT | MIN | MEAN | MAX | N | MIN | MEAN | MAX | N | |
| 1 | -8.8 | -3.3 | -0.3 | 68 | -5.8 | -1.3 | 3.1 | 66 | |
| 2 | -9.8 | -5.5 | -1.3 | 73 | -10.5 | -3.7 | 0.6 | 78 | |
| 3 | -9.7 | -4.1 | 2.2 | 74 | -4.5 | -1.0 | 5.3 | 82 | |
| 4 | -7.8 | -2.0 | 3.4 | 64 | -9.6 | -0.6 | 4.0 | 61 | |
| 5 | -7.1 | -1.9 | 2.9 | 66 | -6.3 | -0.3 | 5.4 | 84 | |
| 6 | -6.7 | -1.7 | 2.5 | 56 | -5.4 | -0.4 | 3.8 | 64 | |

3 Qualitative description

The description of the (reduced) data set is focussed on the VV polarised radar backscatter of the three main crops beet, potato and wheat. The differences between the VV and HH backscatter are only small and for a general description the interpretation of one state of polarization suffices.

The description will take into account:

- The angular behaviour of the radar backscatter for the different crop types (§ 3.1).
- The discrimination of the different crop types by the different frequencies (§ 3.2).
- The temporal behaviour of the radar backscatter in different frequencies for the different crop types (§ 3.3).

3.1 Angular behaviour.

The angular behaviour of the radar backscatter of the three crop types is presented for sortie 1 and sortie 4 in figures 15-20.

For each crop type the angular dependency of the radar backscatter is smooth (there are no fluctuations in the order of several dB that were present in the original, compressed data set). At sortie 1, the radar backscatter decreases a little (3-5 dB) in all frequencies with increasing angle of incidence. At sortie 4, the curves are more or less horizontal.

The crop types are nicely clustered in all frequency bands. Even at sortie 1, when the fields of beet and potato are still bare, the three 'crop types' are often clustered (with or without overlap with other clusters). The clustering at this sortie must then be caused by crop-specific cultivation practices of the soil. For instance the bare soil of potato with its ridges (parallel to the incident radar beam) has a lower backscatter than that of beet in all three frequency bands and at all angles of incidence. Only in the S-band are the fields of wheat at sortie 1 spread amongst the clusters of beet and potato.

At sortie 4, there is a large gap between the clusters of beet and potato on the one hand, and that of wheat on the other. At all frequencies and angles of incidence, the backscatter of wheat is some 5-8 dB lower than that of beet and potato. In the L-band, there is also some 3 dB difference between beet and potato; the backscatter of potato being higher than that of beet. In the S-band, these clusters are closer together while in the Ku1-band they fully overlap.

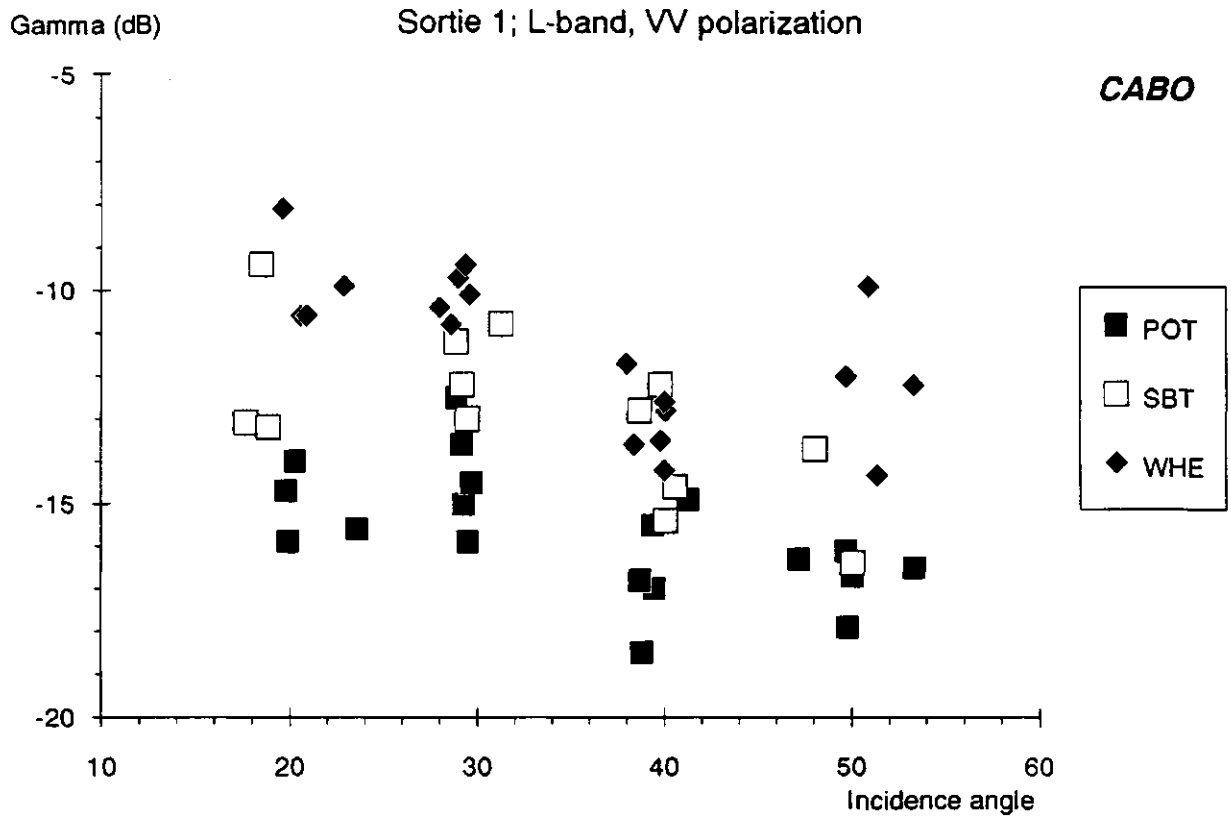


Fig. 15 Radar backscatter of 'beet-soil', 'potato-soil' and 'wheat-soil' (sortie 1, L-band, VV) as a function of incidence angle

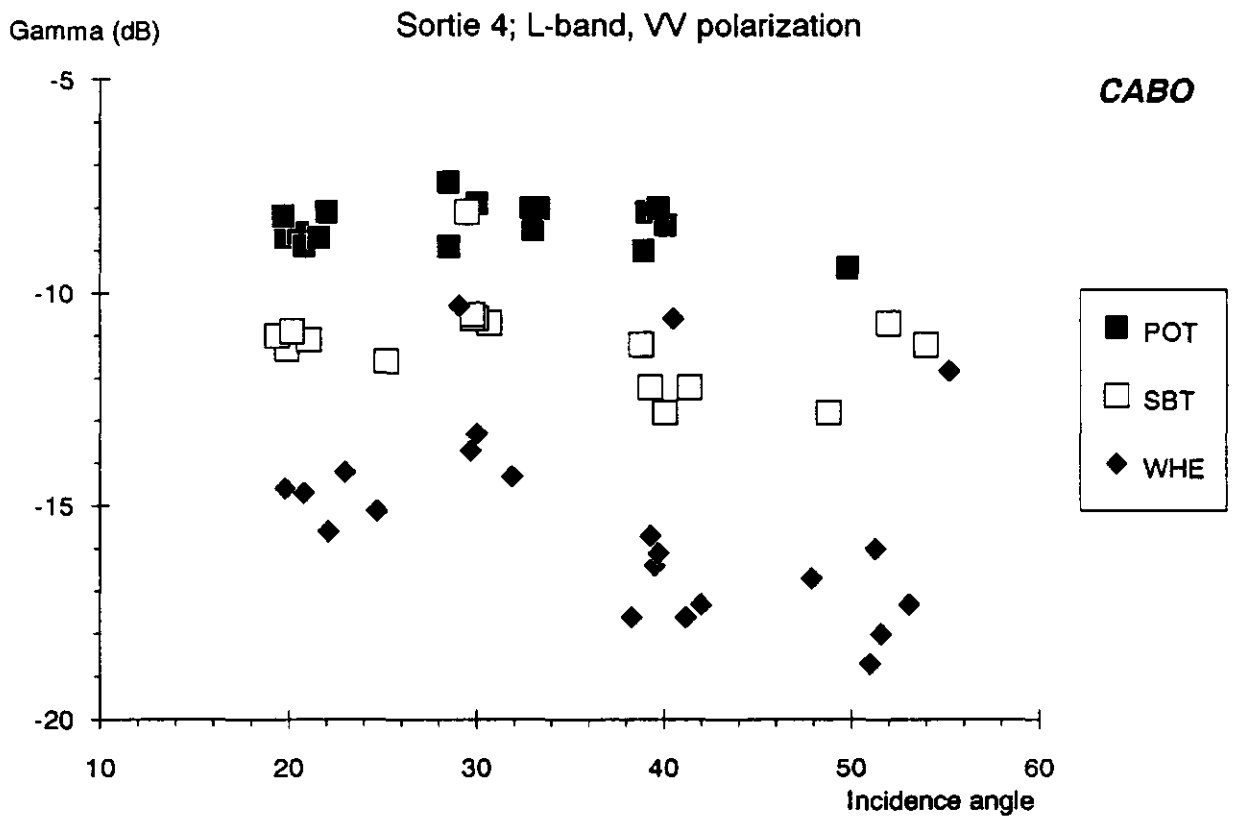


Fig. 16 Radar backscatter of beet, potato and wheat (sortie 4, L-band, VV) as a function of incidence angle

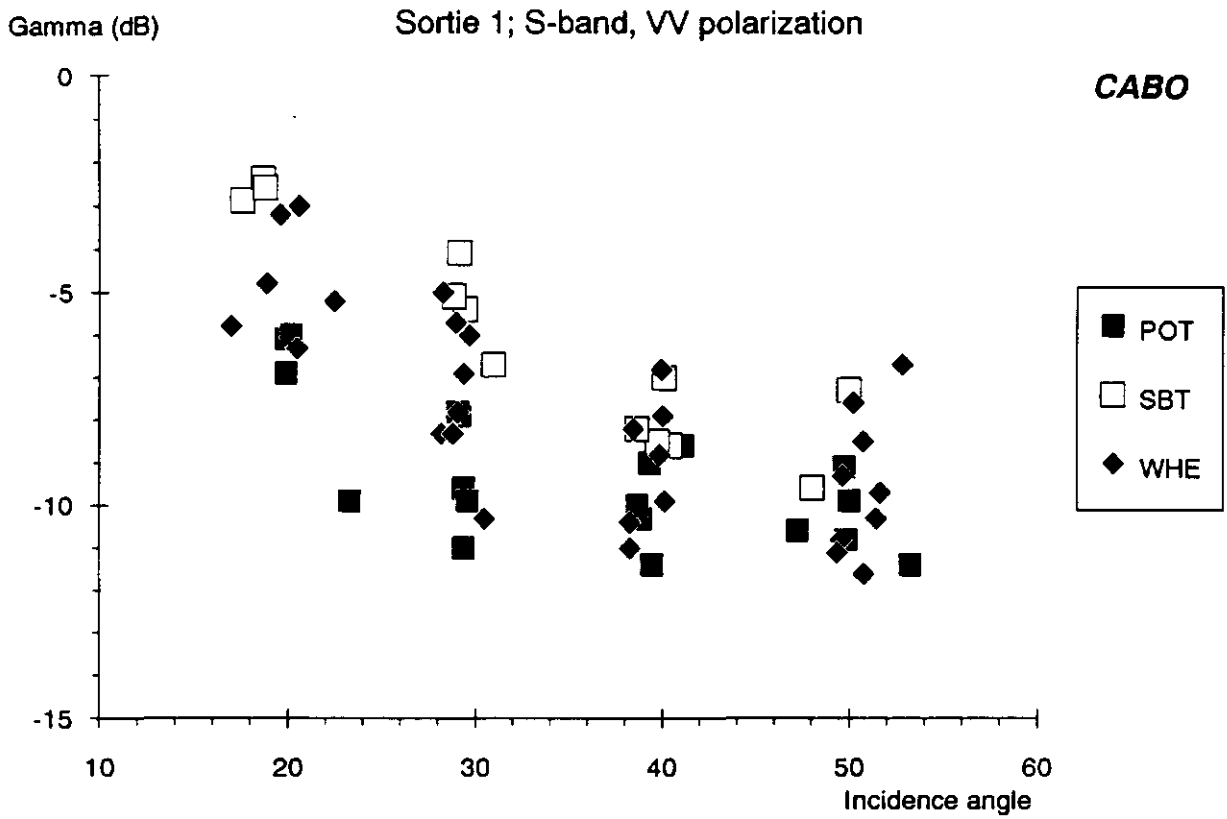


Fig. 17 Radar backscatter of 'beet-soil', 'potato-soil' and 'wheat-soil' (sortie 1, S-band, VV) as a function of incidence angle

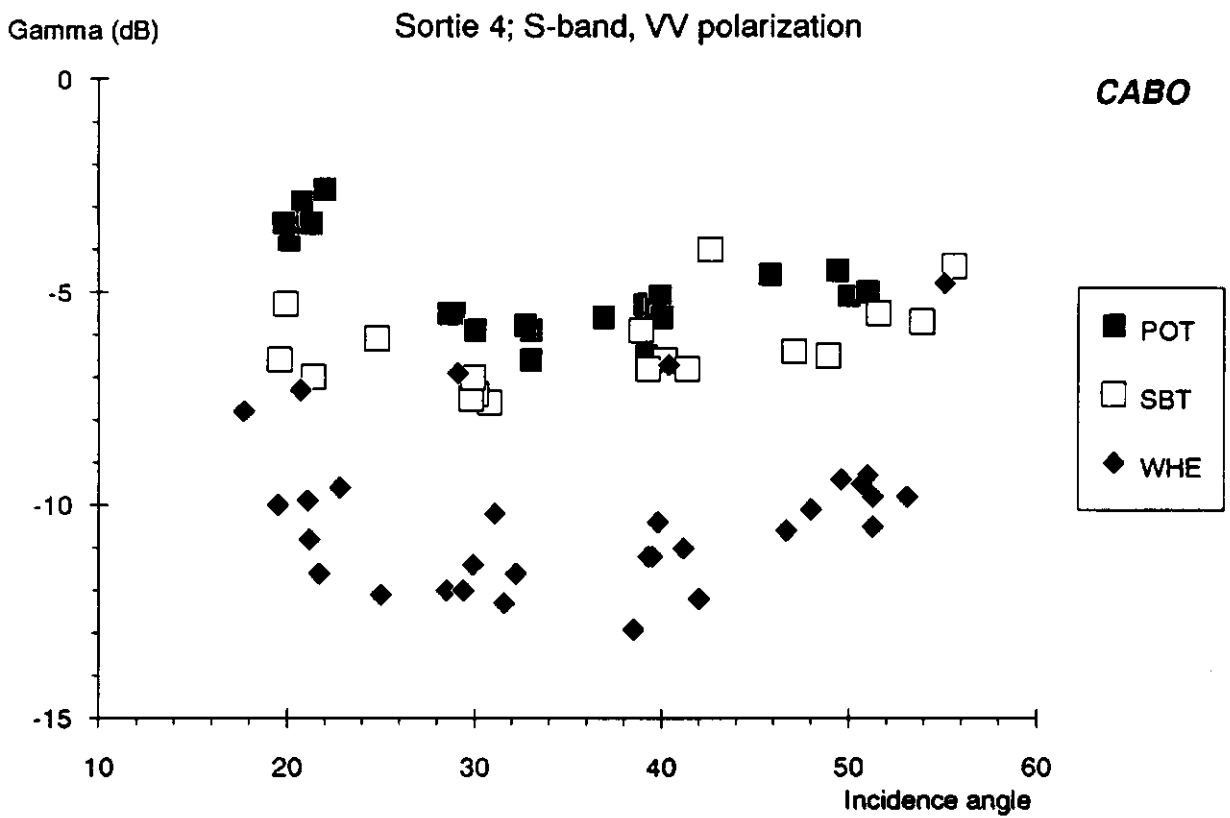


Fig. 18 Radar backscatter of beet, potato and wheat (sortie 4, S-band, VV) as a function of incidence angle

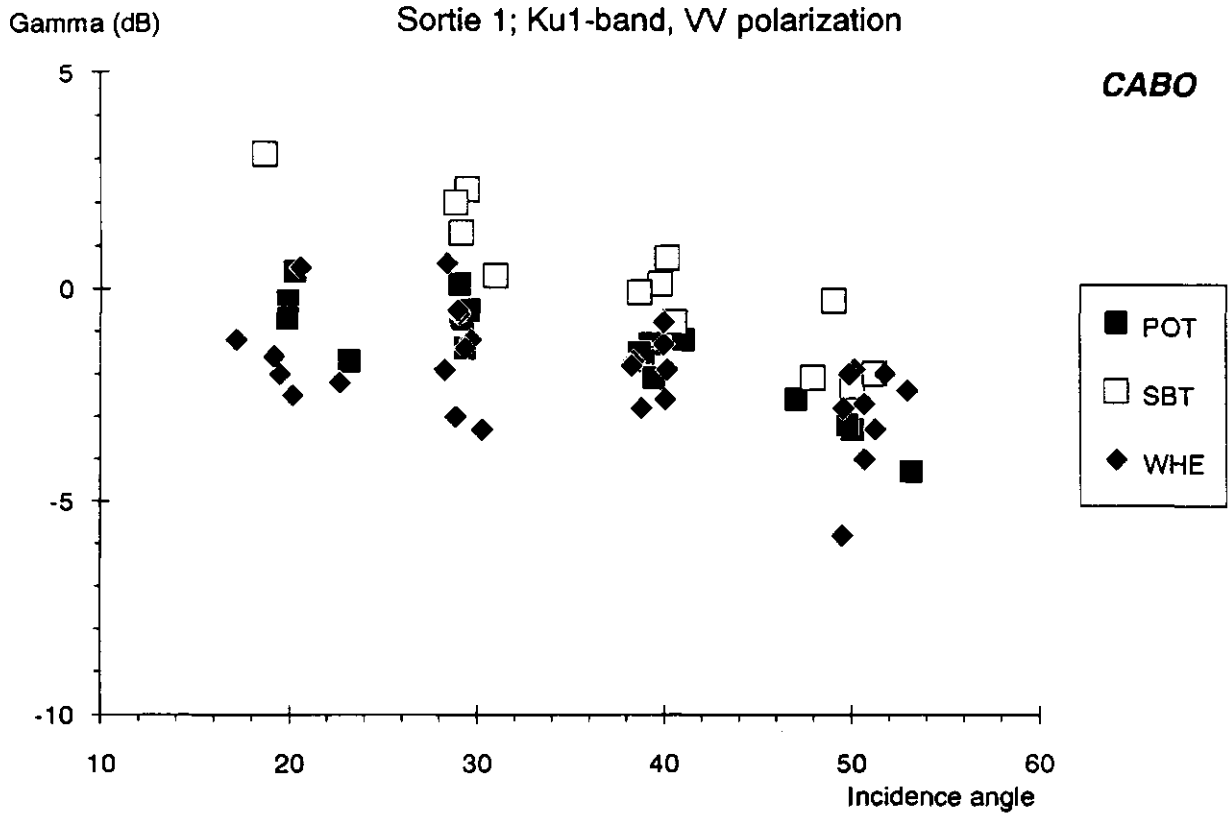


Fig. 19 Radar backscatter of 'beet-soil', 'potato-soil' and 'wheat-soil' (sortie 1, Ku1-band, VV) as a function of incidence angle

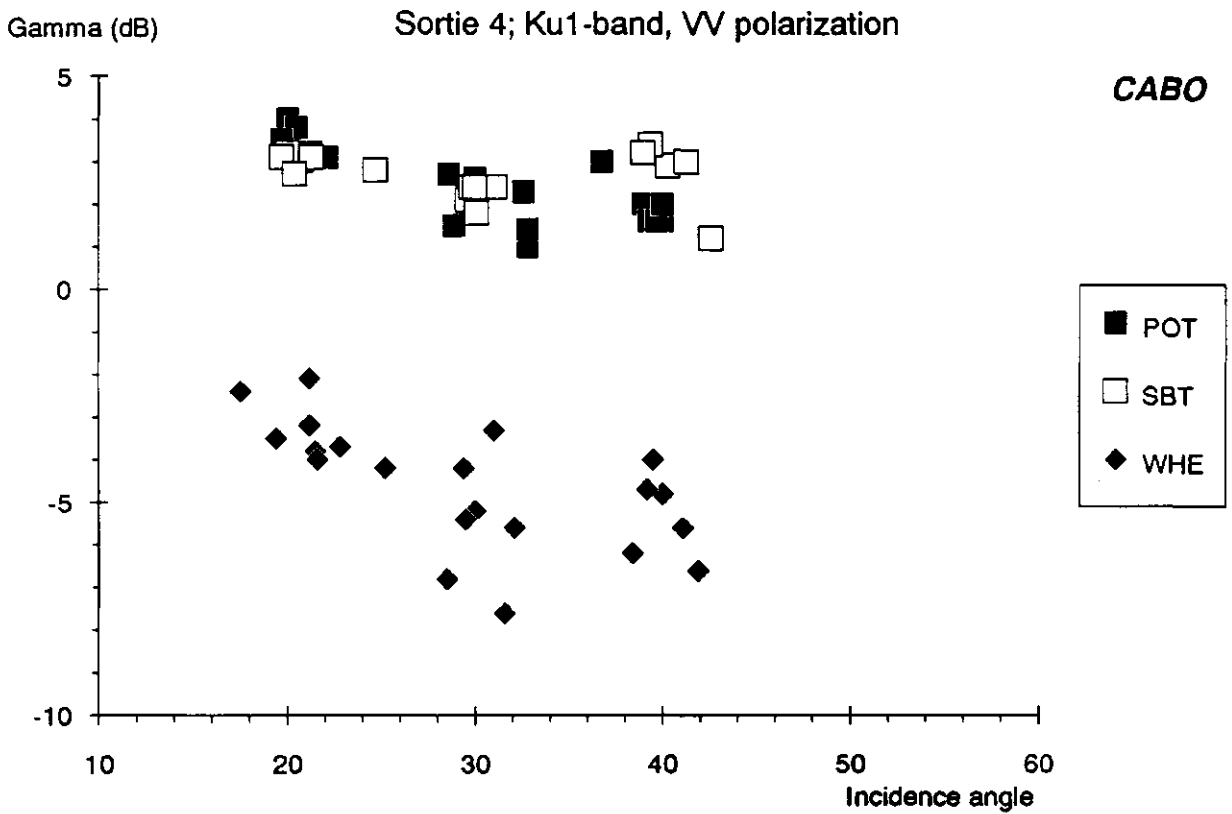


Fig. 20 Radar backscatter of beet, potato and wheat (sortie 4, Ku1-band, VV) as a function of incidence angle

3.2 Crop type discrimination.

From the previous paragraph it is clear that each frequency band offers some possibilities for crop type discrimination. From the figures it is derived that a combination of several incidence angles in a single frequency band will not improve discrimination possibilities over a single incidence angle in a single frequency band. If discrimination possibilities in one sortie are to be improved, this must be found in a combination of frequency bands. Clusters of crop types in two frequency bands can be visualized in feature space plots, figures 21-26. Combinations are made here of the L-S, L-Ku1 and S-Ku1 bands for mainly bare soil (sortie 1) and crops (sortie 4). Based on the figures 15-20, the data at the incidence angles 20° and 30° are lumped for sortie 4, while for sortie 1 only data at 30° incidence angle are selected.

For mainly bare soil, the combination of the L- and the Ku1-band offers the best potentials. The L-band separates 'potato-soil' from 'beet-' and 'wheat-soil' (70% crop cover), and the Ku2-band separates 'beet-soil' from 'potato-' and 'wheat-soil' (70% crop cover). The S-band can distinguish between 'beet-' and 'potato-soil', but the cluster of 'wheat-soils' (70% crop cover) encompasses both the other 'crop-soils'.

For crops, the most important band is the L-band, and the best combination is with the S-band. In all three bands, wheat is very well separated from beet and potato, but only in the L-band (and to some extent in the S-band) potato is separated from beet. In all bands, the trends are similar so that clusters in the feature space plots lie more or less on a 45° line.

In the two plots with the S-band, two groups of potato appear which are not present in the third plot (L-Ku2 plot). This is the result of the lumping of the measurements at 20° and 30° incidence angle in which there is a difference of about 3 dB for potato only, figure 18. This specific example illustrates the care that must be taken in the general lumping of backscatter measurements.

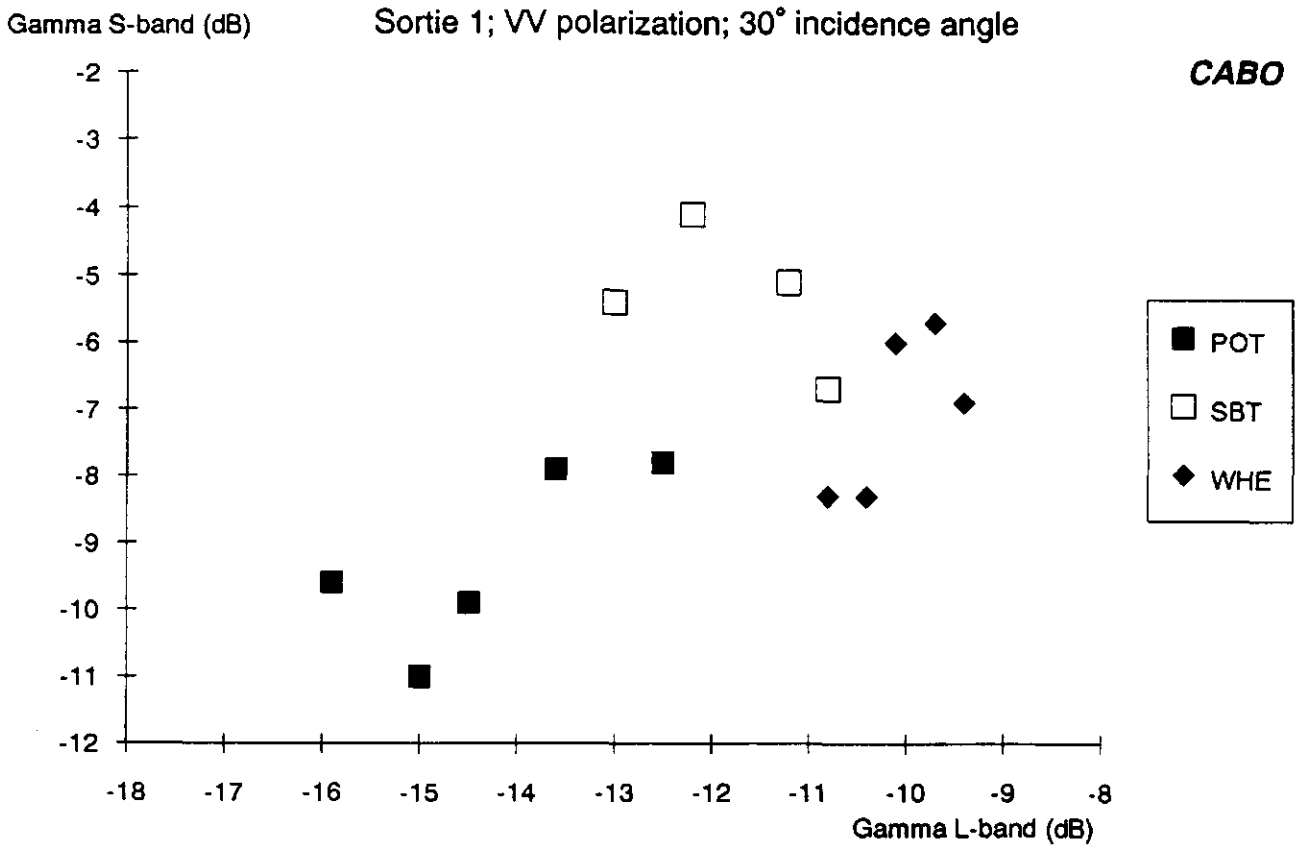


Fig. 21 Feature space plot (sortie 1, VV, 30° i.a.) of the S-band versus the L-band of 'beet-soil', 'potato-soil' and 'wheat-soil'

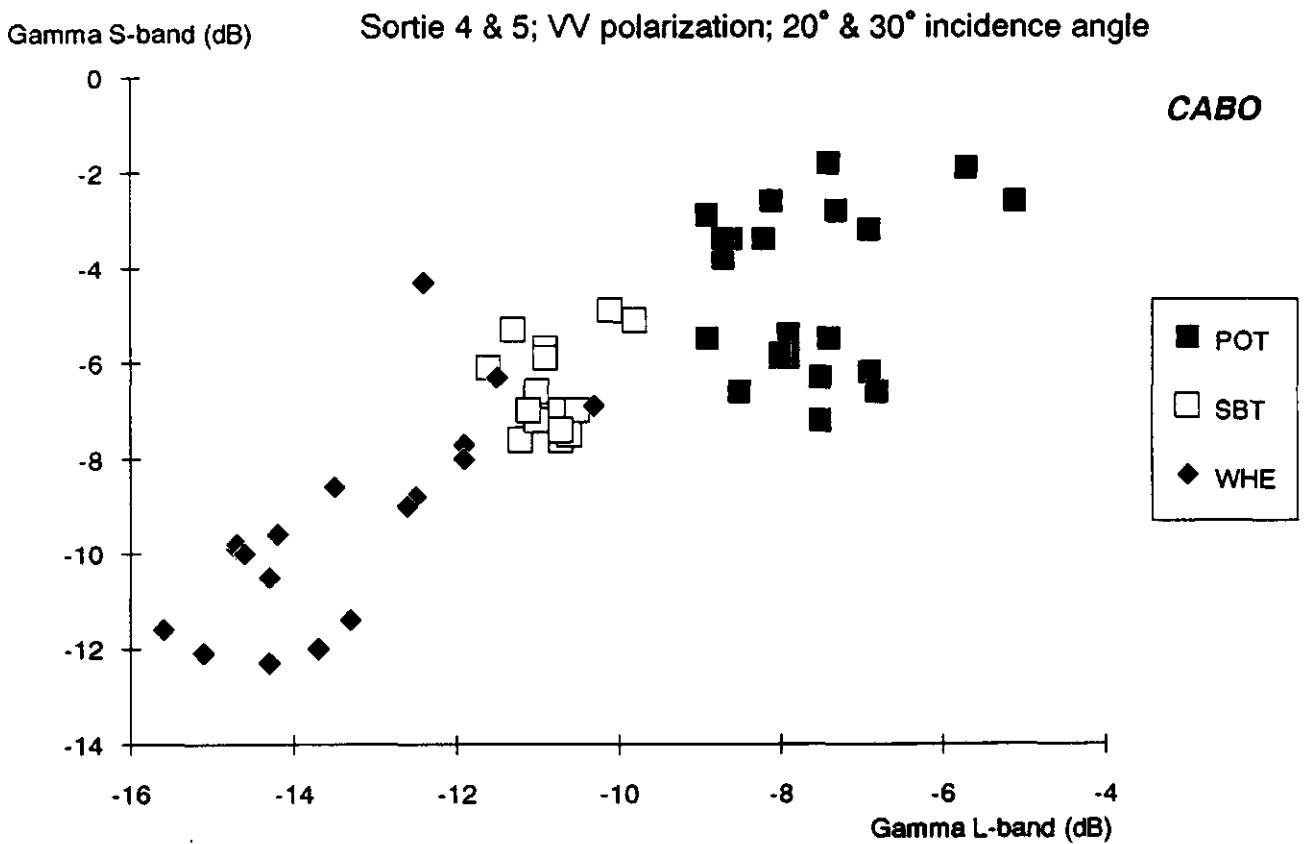


Fig. 22 Feature space plot (sortie 4 & 5, VV, 20° & 30° i.a.) of the S-band versus the L-band for potato, beet and wheat

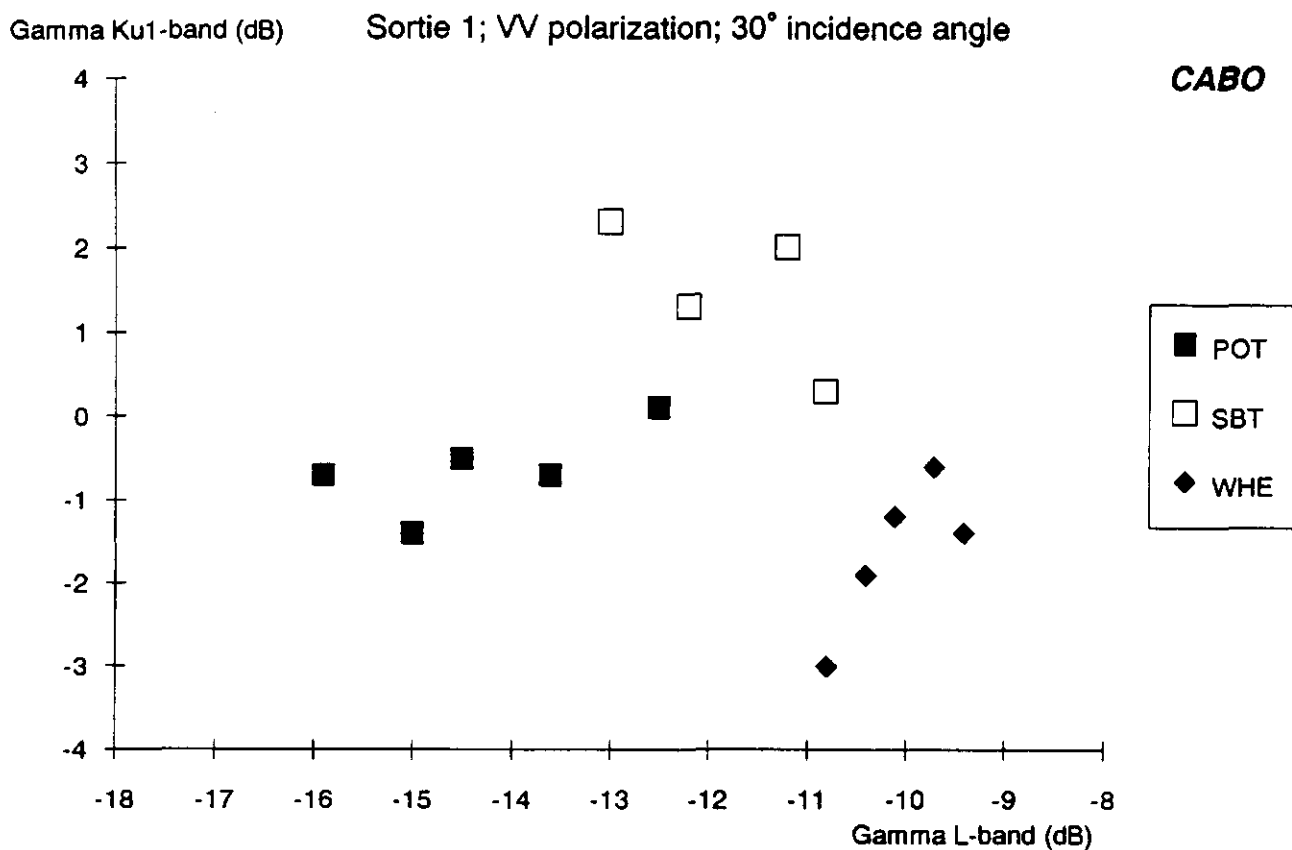


Fig. 23 Feature space plot (sortie 1, VV, 30° i.a.) of the Ku1-band versus the L-band of 'beet-soil', 'potato-soil' and 'wheat-soil'

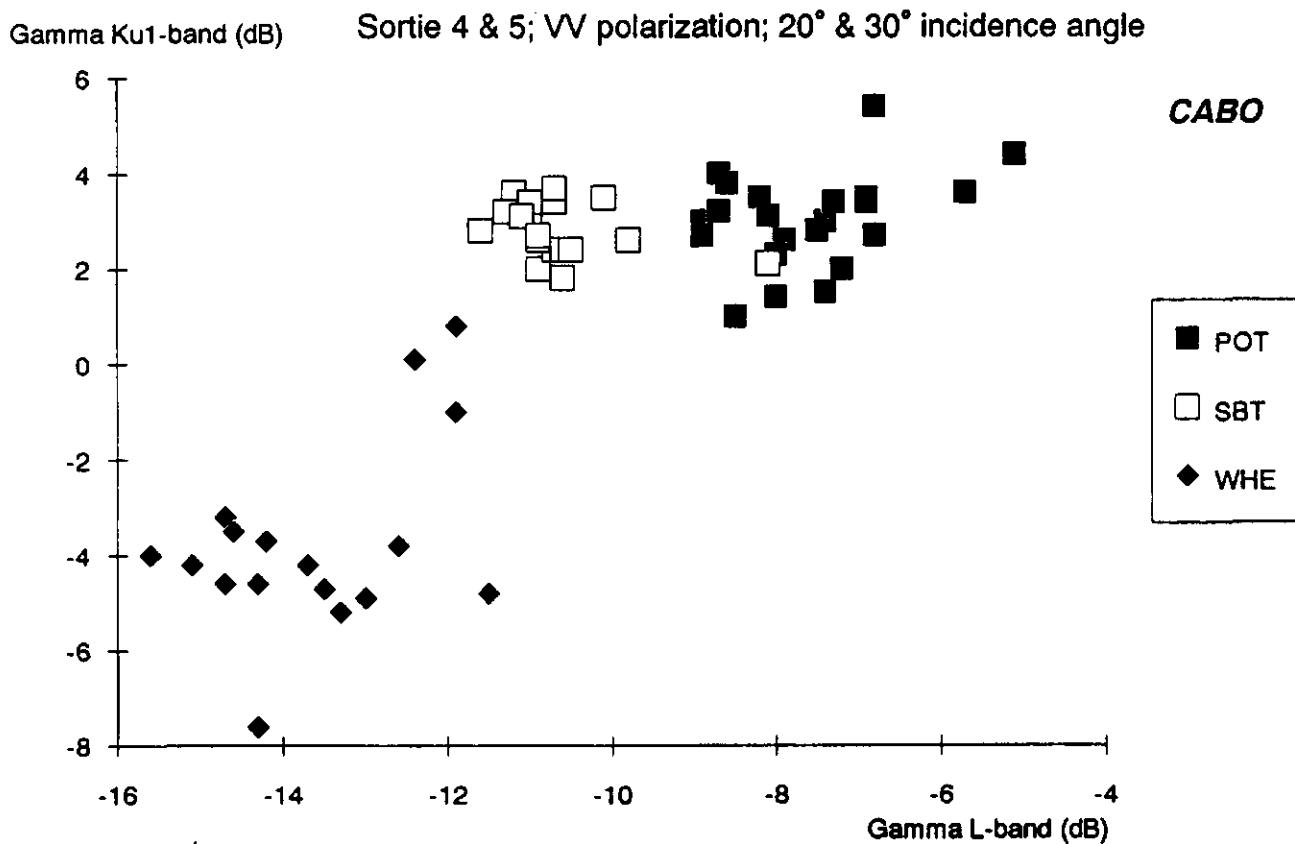


Fig. 24 Feature space plot (sortie 4 & 5, VV, 20° & 30° i.a.) of the Ku1-band versus the L-band for potato, beet and wheat

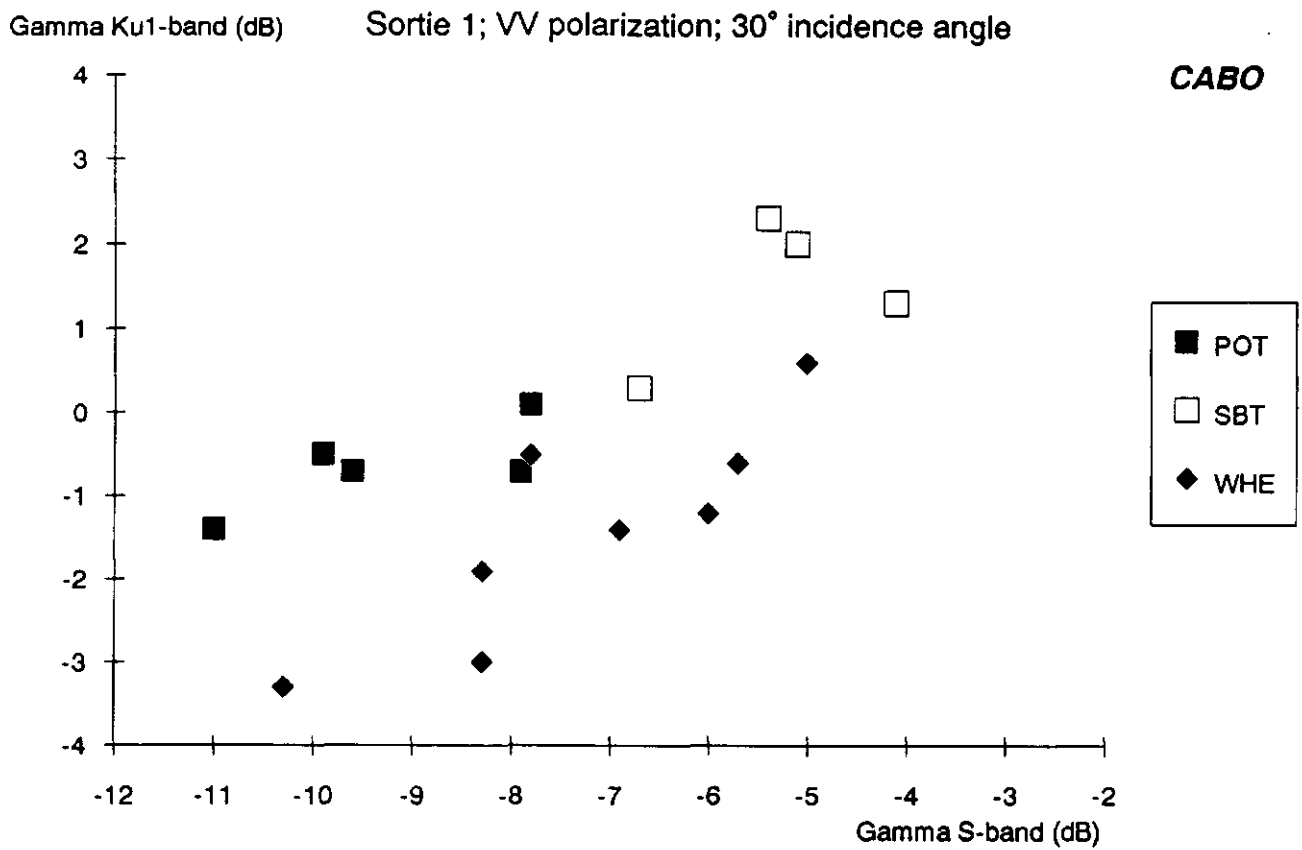


Fig. 25 Feature space plot (sortie 1, VV, 30° i.a.) of the Ku1-band versus the S-band of 'beet-soil', 'potato-soil' and 'wheat-soil'

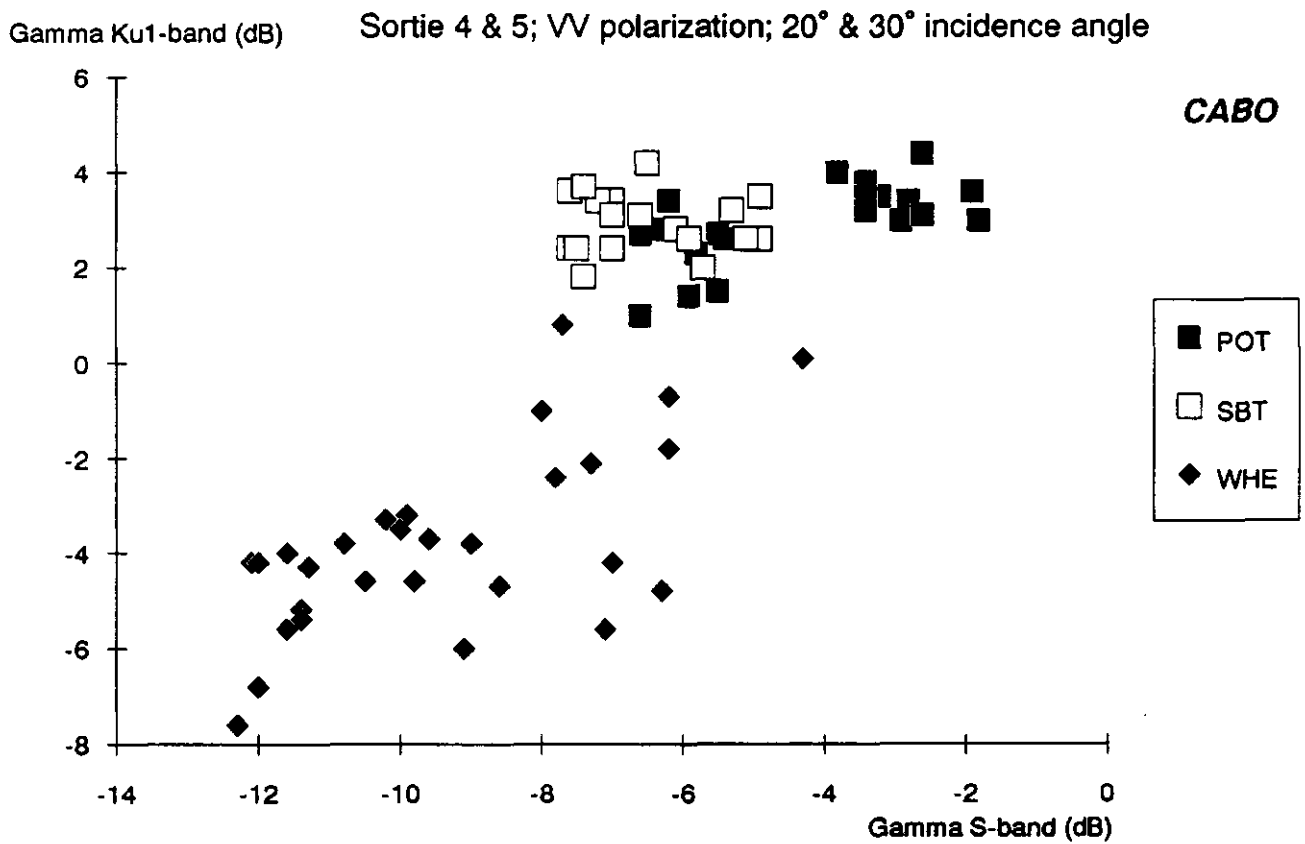


Fig. 26 Feature space plot (sortie 4 & 5, VV, 20° & 30° i.a.) of the Ku1-band versus the S-band for potato, beet and wheat

3.3 Temporal behaviour.

For the three main crop types, the change in the radar backscatter in time (VV polarised; 40° incidence angle) is plotted together with the growth of the crops expressed by crop cover (expressed in fraction), dry biomass and Leaf Area Index (LAI), figures 27-35. The average moisture content of the top soil (0-5 cm) at the different sorties is plotted in figure 36.

A description is made of the radar backscatter per crop type. Some reference is made to the ROVE data set of ground based X- and Q-band measurements on small test fields (Bouman 1987, Bouman and van Kasteren 1989).

Beet:

At all sorties, the individual fields are nicely clustered in all frequency bands.

A remarkable feature is the dip in the radar backscatter in both the L- and the Ku1-band at sortie 2 (day 152). It is not only present at 40° incidence angle, but also at 20° and 30° with similar magnitude, 3-4 dB. Only at 50° this dip is smaller, about 1-2 dB.

This dip of 3-4 dB can only to some extent be explained by field observations. The moisture content of the beet fields decreases from an average 35.5% at sortie 1 to an average 29.5% at sortie 2. Though this is a decrease of 5%, the moisture content is still very high at both sorties. The growth of the beet between these sorties is only small (expressed in plant water: an average of 0.010 at sortie 1 to an average of 0.122 kg/m² at sortie 2). However, any growth in this period is only expected to lead to an increase in radar backscatter rather than to a decrease (ROVE database X- and Q-band; the increase in backscatter after sortie 2). A short calculation with the cloud formula for beet with these values for plant water and soil moisture content, and based on the parameters derived from the ROVE experiment on De Schreef yields the following results for the X-band:

- Sortie 1: $\gamma = -0.97$ dB
- Sortie 2: $\gamma = -2.22$ dB

Though a decrease in backscatter is predicted, the order of magnitude is more around 1.2 dB than the measured 3.5 dB for the Ku1-band (which is close to the X-band).

After sortie 2 the radar backscatter increases in all three frequency bands with the further growth of the crop:

- in L-band γ increases 4 dB until sortie 3 (cover: 0.30, biomass: 500 kg/ha, LAI: 1)
- in S-band γ increases 2 dB until sortie 4 (cover: 0.82, biomass: 2250 kg/ha, LAI: 2.5)
- in Ku1-band γ increases 6 dB until sortie 4 (cover: 0.82, biomass: 2250 kg/ha, LAI: 2.5)
(comparison with X-band ROVE dataset: γ increases 8 dB)

The backscatter thus saturates at a relative early stage of growth, cover: 0.30-0.82, biomass: 50-2250 kg/ha, LAI: 1-2.5. The growth of beet increases further, cover: 0.97, biomass: 4350 kg/ha, LAI: 5, but this is not registered by the radar backscatter in any of the frequency bands. The best band for monitoring growth seems to be the Ku1-band.

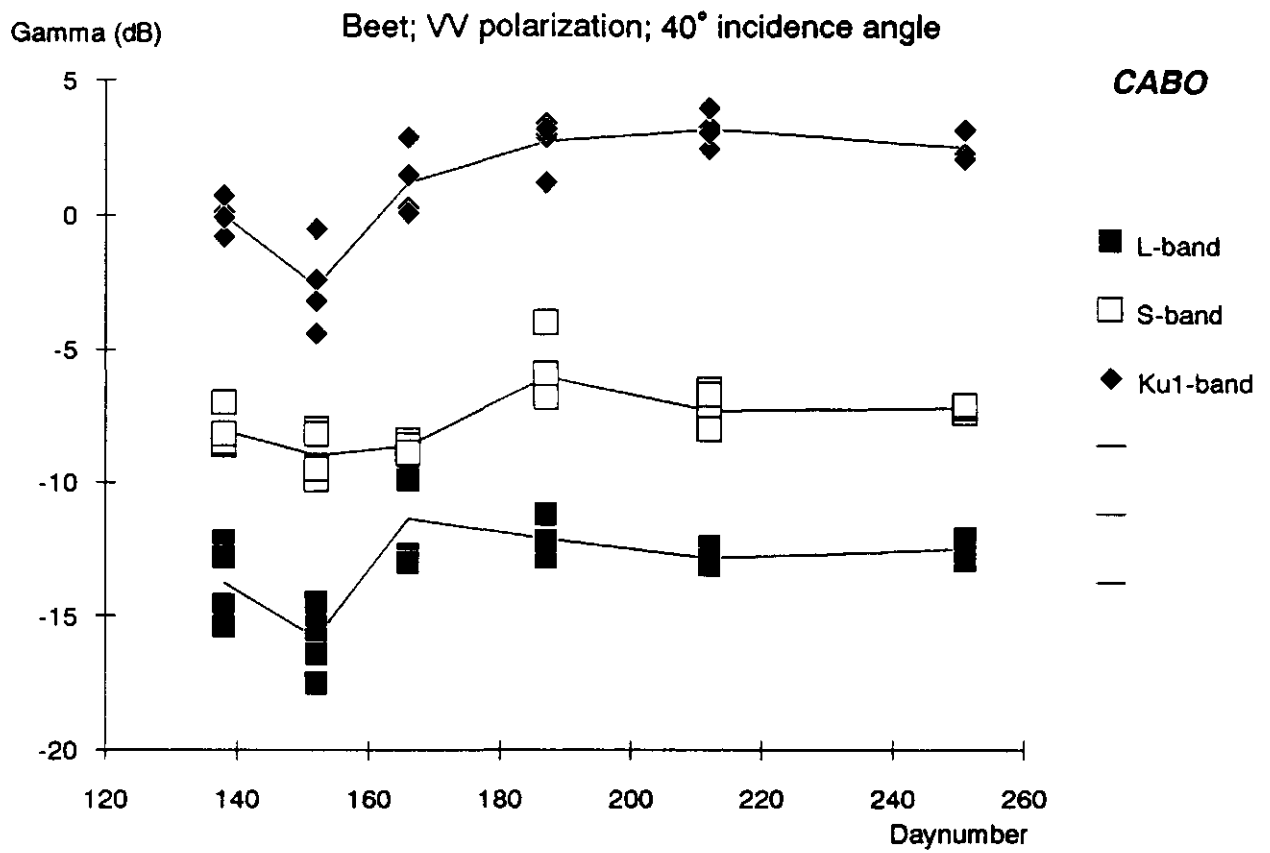


Fig. 27 Radar backscatter of beet (L-, S-, Ku1-band, VV, 40° i.a.) in the course of the growing season

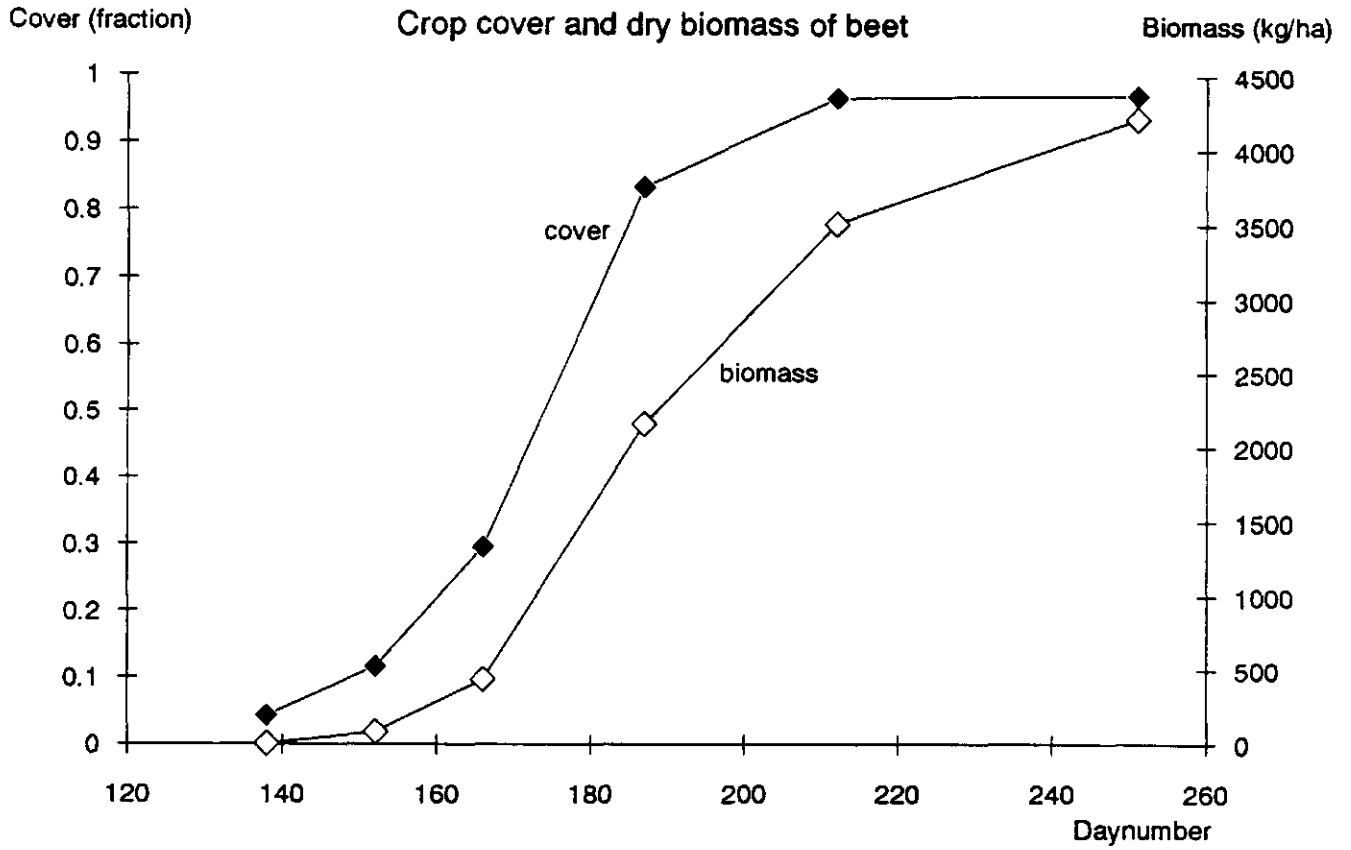


Fig. 28 Crop cover and dry biomass of beet in the course of the growing season, averaged for all fields

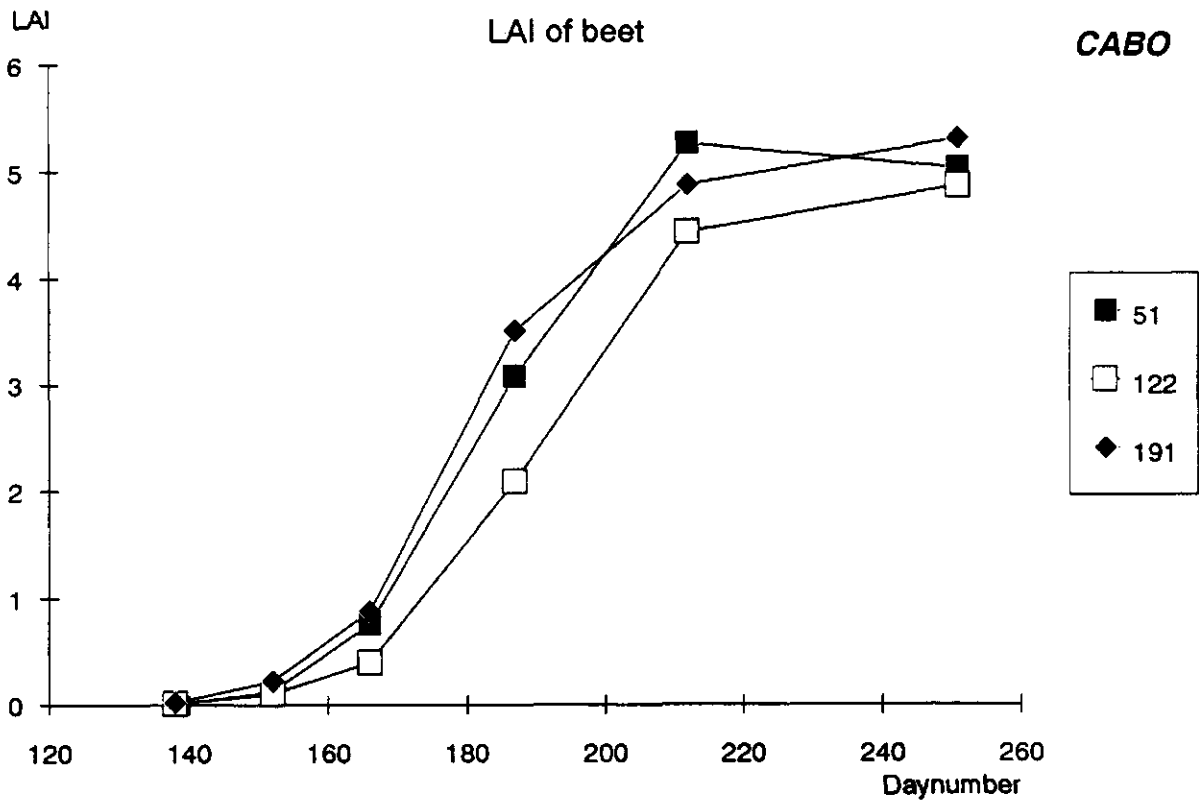


Fig. 29 Leaf Area Index (LAI) of beet in the course of the growing season, the numbers in the legend refer to the fieldnumbers of the crops

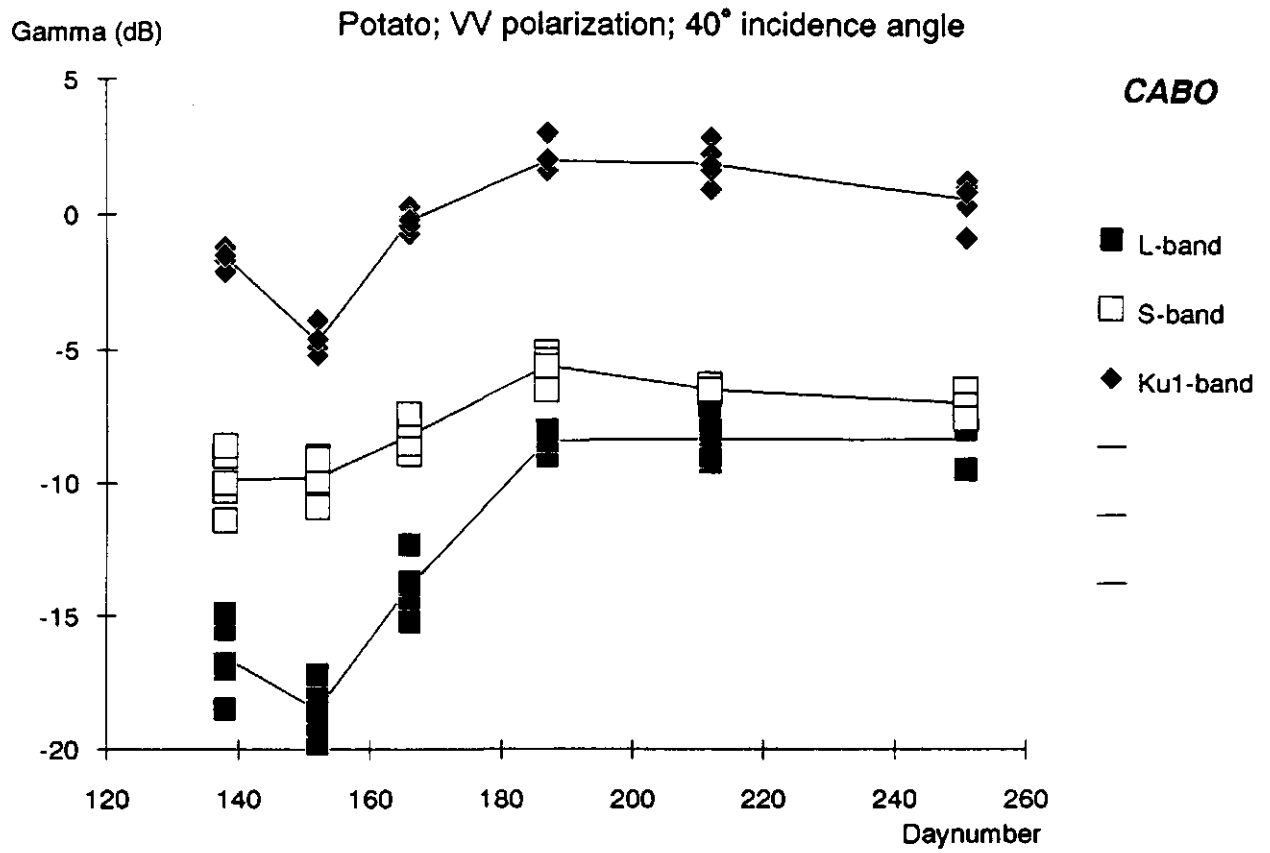


Fig. 30 Radar backscatter of potato (L-, S-, Ku1-band, VV, 40° i.a.) in the course of the growing season

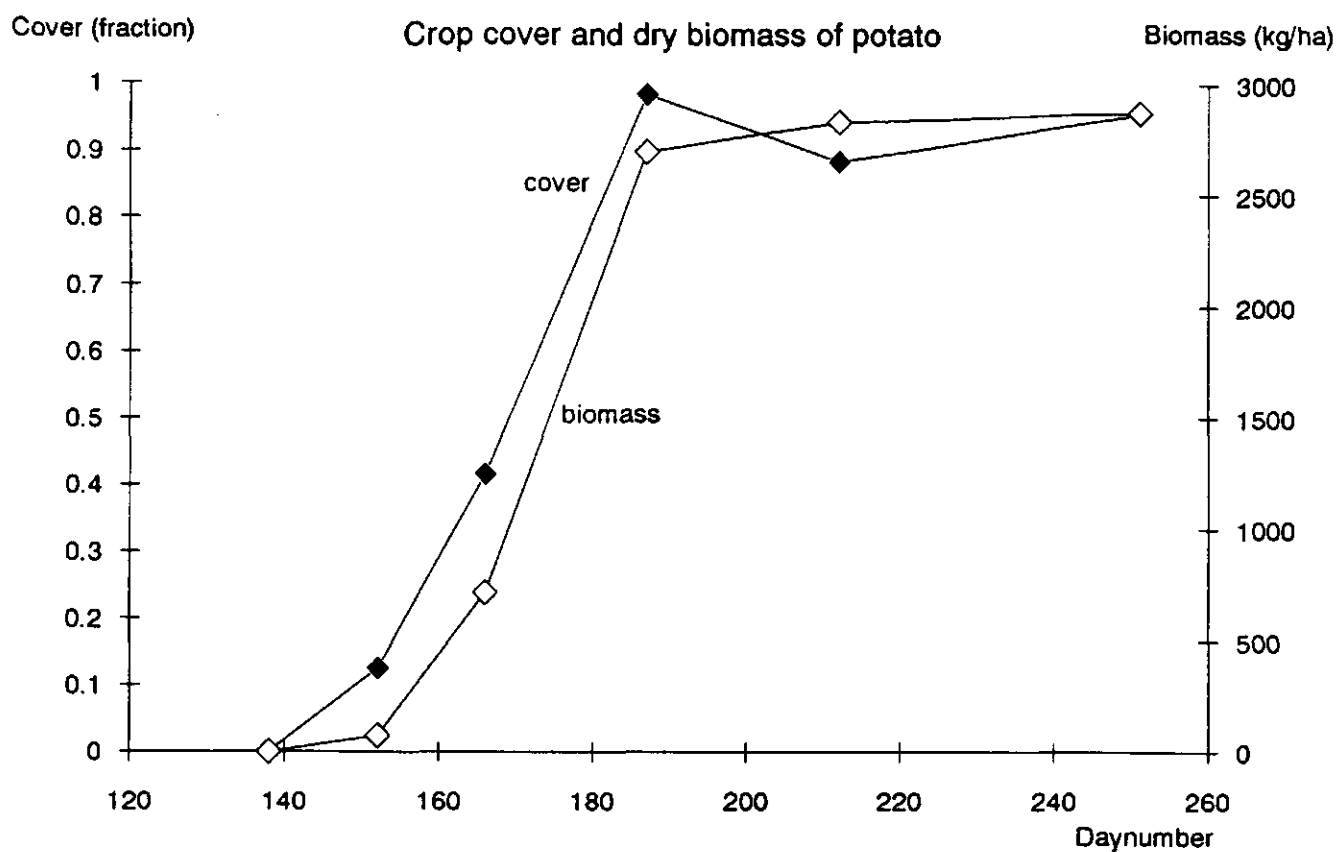


Fig. 31 Crop cover and dry biomass of potato in the course of the growing season, averaged for all fields

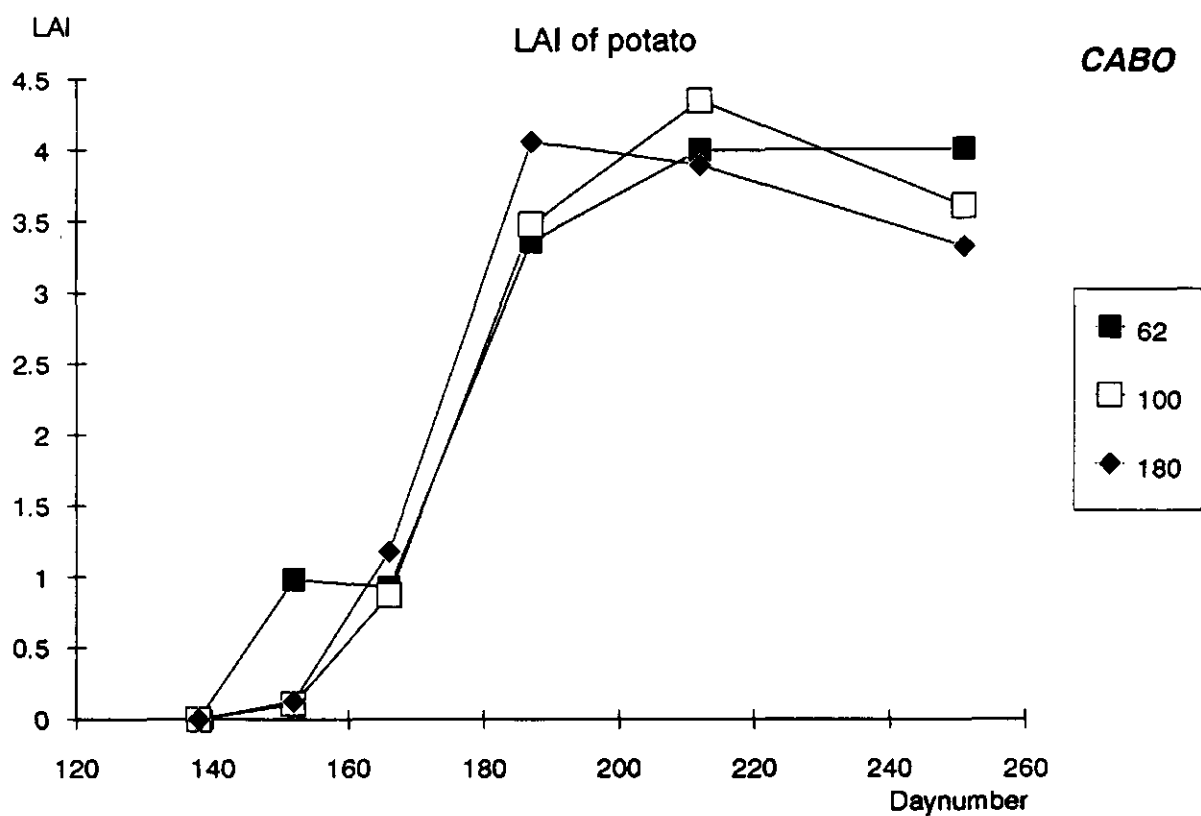


Fig. 32 Leaf Area Index (LAI) of potato in the course of the growing season, the numbers in the legend refer to the fieldnumbers of the crops

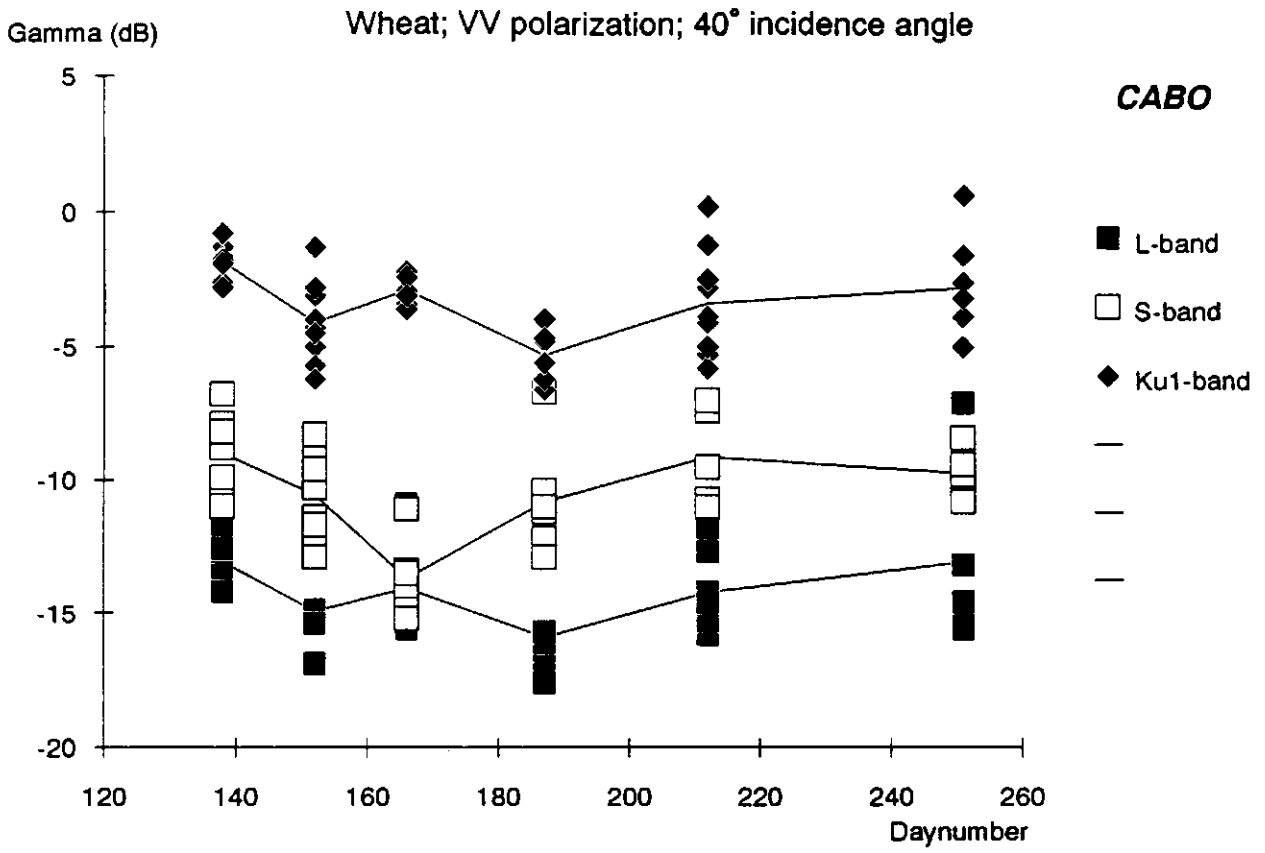


Fig. 33 Radar backscatter of wheat (L-, S-, Ku1-band, VV, 40° i.a.) in the course of the growing season

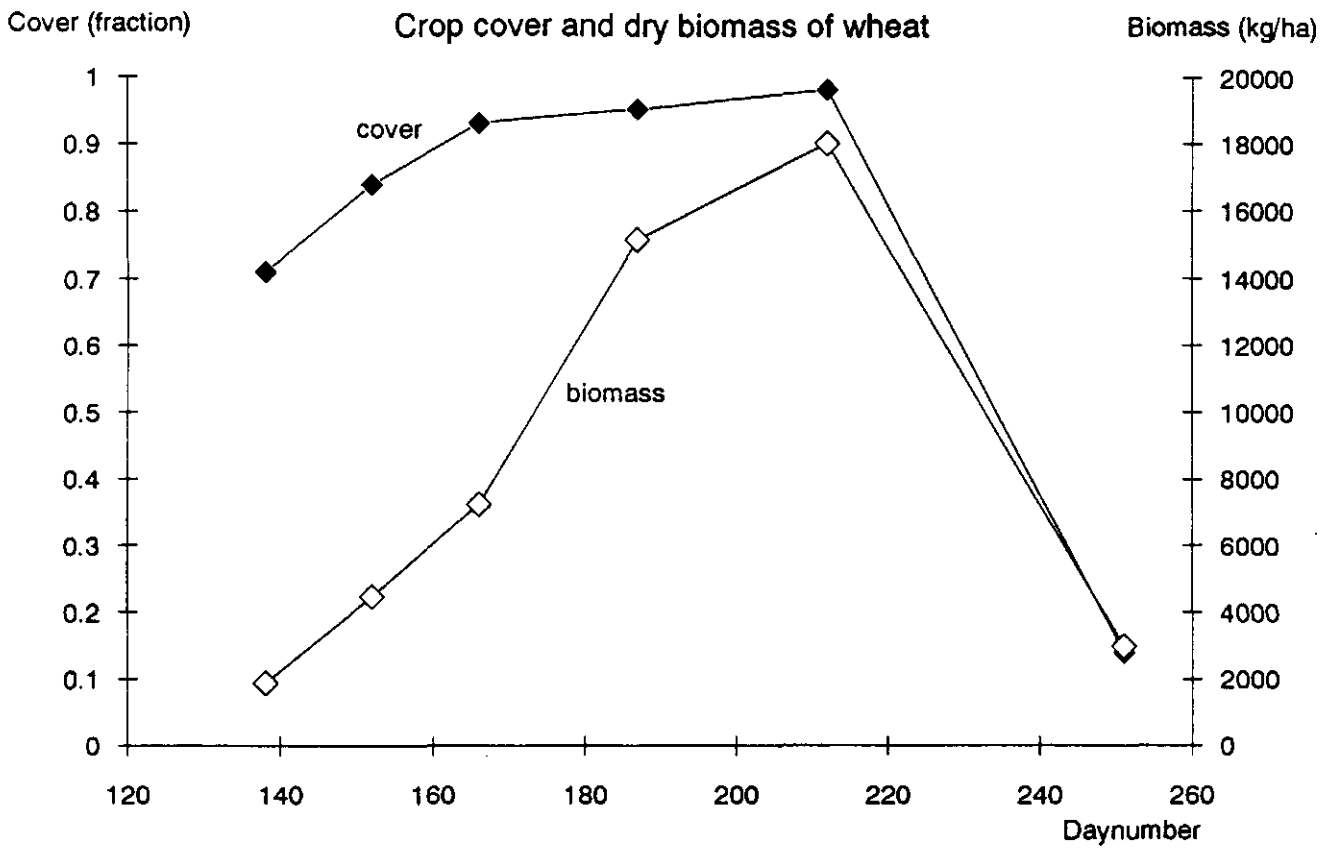


Fig. 34 Crop cover and dry biomass of wheat in the course of the growing season, averaged for all fields

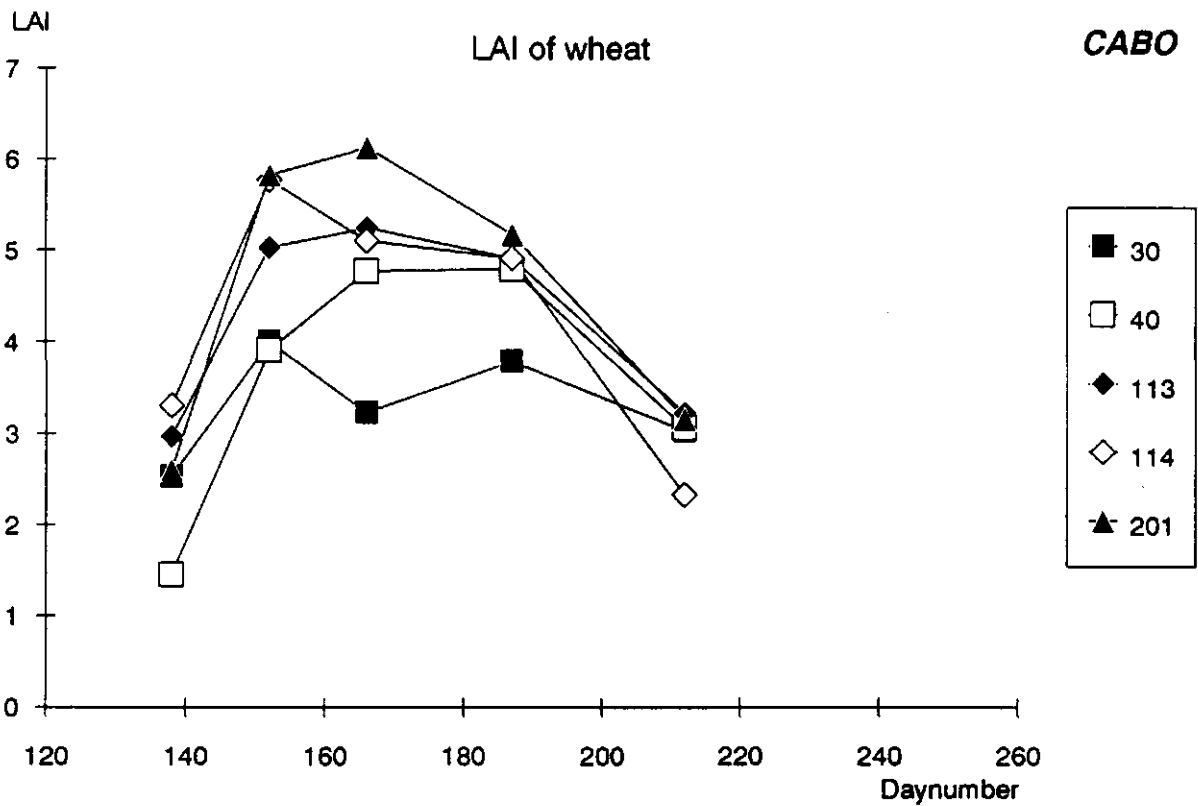


Fig. 35 Leaf Area Index (LAI) of wheat in the course of the growing season, the numbers in the legend refer to the fieldnumbers of the crops

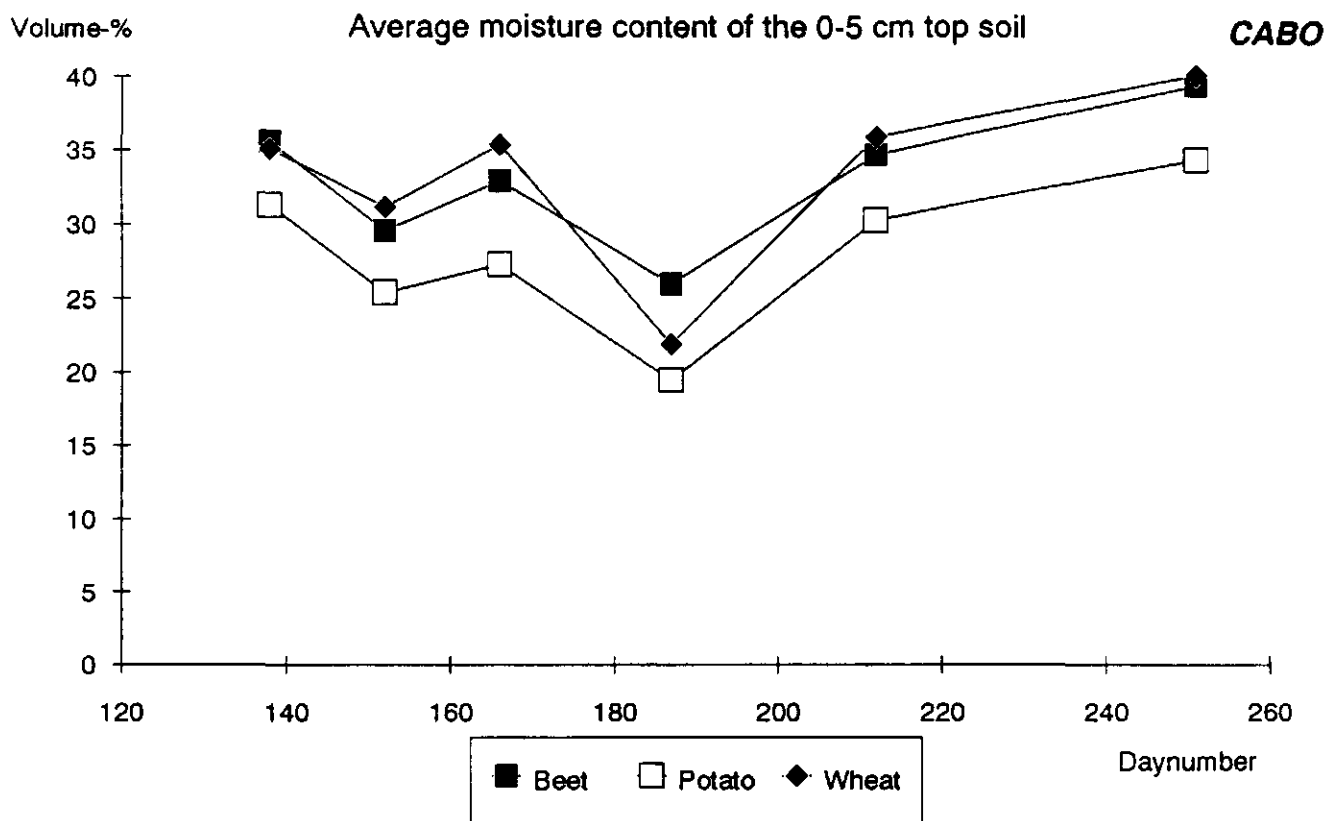


Fig. 36 Average moisture content of the top soil (0-5 cm) of beet, potato and wheat in the course of the growing season

Like in the track plots of paragraph 2.1, the dynamics in the S-band are smaller than in the other two bands. When compared to the ROVE data, the dynamics in the Ku1-band are lower than in the ROVE-X-band.

When the temporal radar backscatter of beet is compared with the changes in the soil moisture content, figure 36, there seems to be no correlation. Only the decrease in moisture content at sortie 2 might be recognized in the backscatter curves (discussion above). The larger dip in moisture content at sortie 4 (fully grown crop canopy), however, is not recognized at any of the frequency bands. Apparently, the microwaves can not penetrate the crop canopy. Even the backscatter in the L-band, in which the microwaves could theoretically penetrate the canopy better than in higher frequency bands, does not react on this dip.

Potato:

Like for beet, the individual fields are nicely clustered. Also, the curves of the L- and Ku1-band are characterised by a dip of 3-4 dB at sortie 2. After sortie 2 the backscatter increases in all frequency bands:

- in L-band γ increases 10 dB until sortie 4 (cover: 0.97, biomass: 2750 kg/ha, LAI: 3.5)
 - in S-band γ increases 4 dB until sortie 4 (cover: 0.97, biomass: 2750 kg/ha, LAI: 3.5)
 - in Ku1-band γ increases 6 dB until sortie 4 (cover: 0.97, biomass: 2750 kg/ha, LAI: 3.5)
- (comparison with X-band ROVE dataset: γ increases 4 dB)

The general shapes of the temporal curves resemble those of beet. Remarkably, however, is the large increase in the L-band of 10 dB compared to that of 4 dB for beet (no explanation for this is found yet). Also in the S-band, the increase for potato is larger than for beet (though less pronounced), while in the Ku1-band, it is similar. In this latter band, the increase is larger than in the ROVE-X-band. Like for beet, the total dynamics are lowest in the S-band.

Since the growth of potato reaches maximum values, cover: 0.97, biomass: 2750 kg/ha, LAI: 4, in a relative early stage of the growing season (compared to beet), the possibilities for monitoring growth appear better. The best band for monitoring potato-growth seems to be the L-band.

Like for beet, there seems to be no correlation between the radar backscatter in time and the soil moisture content (except possibly for the dip at sortie 2). Despite the decrease in moisture content at sortie 4, the radar backscatter increases in all frequency bands.

Wheat:

The curves of wheat differ from those of beet and potato. Again, there is a dip in the radar backscatter in the L- and the Ku1-band, but it is much less pronounced since the backscatter generally decreases further until sortie 4. At sorties 5 and 6, the backscatter then increases again with some 3 dB. In the S-band, the backscatter continually decreases until sortie 3, after which it returns with some 4 dB to its original level. On visual comparison, the backscatter appears correlated with the LAI: decreasing backscatter with increasing LAI until sortie 3, and then increasing backscatter with decreasing LAI until harvest. However, the backscatter appears also correlated with the soil moisture content, figure 36. The pattern of the radar backscatter in the L- and the Ku1-band greatly resembles that of the soil moisture in time. The small dip at sortie 2, and the large dip at sortie 4 are faithfully reproduced. The only deviation between the

backscatter and the soil moisture content is at sortie 3 in the S-band. It is therefore not unambiguous whether the temporal curves of the radar backscatter can be explained by the growth of the crops or by the pattern of the soil moisture content.

Overall, the impression of the temporal curves is a slightly concave one. The average 'growth'-range in all bands is small, about 4 dB only. In the ROVE-X-band, the temporal curves are also hollow: first a decrease with crop growth until the stage of ear-filling, and an increase at the end of the growing season with the ripening of the crop. The average X-band 'growth'-range in backscatter is about 5 dB (Bouman and van Kasteren, 1989).

The spread between the individual fields in each band, and especially in the Ku1- and the S-band, is larger than for beet and potato. This matches the spread between the LAI values which is also larger than for the other crops. (In the ROVE-X-band data set, a large variation in the radar backscatter of wheat is found in relation to crop variety (leaf size, canopy structure, LAI), management practices and weather influences).

General crop comparison:

A general comparison of the crop types in the different frequency bands at 20° and 40° incidence angles is given in figures 37-40. These figures show some small differences between the two angles of incidence. At sortie 2, the backscatter of the potato fields is lower than that of the beet fields in all frequency bands at both angles of incidence (only in the S-band at 40°, there is no difference). When the LAI is maximal, at sortie 5, the backscatter of the potato fields is much higher than that of the beet fields in all three frequency bands at 20° incidence angle. At 40°, this is only true in the L-band while there is hardly any difference in the other bands (compare also the figures in paragraph 3.1; scale differences!).

As remarked before, there is more variation between the backscatter of the wheat fields (especially in the Ku1-band) than between that of the potato and beet fields. At sortie 5, the backscatter of wheat is lower than that of the other crops, especially in the Ku1-band.

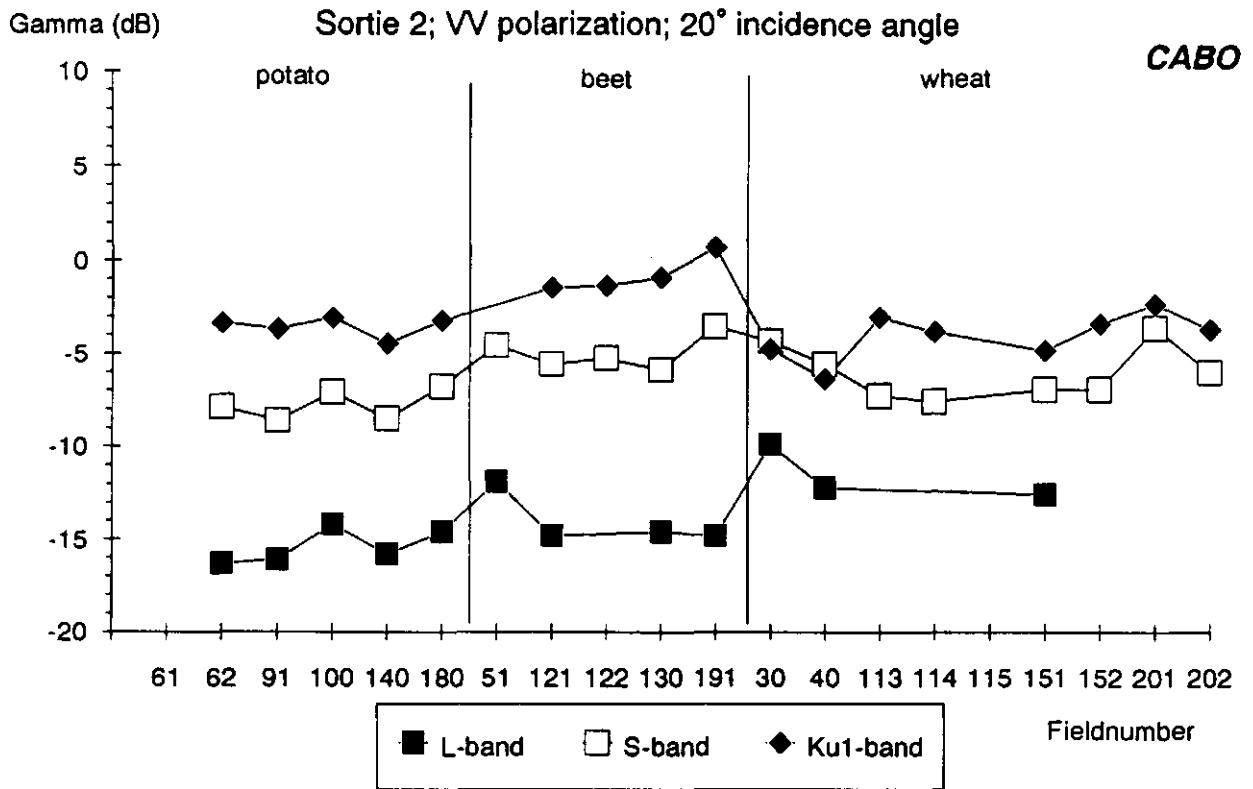


Fig. 37 Radar backscatter of the main croptypes (sortie 2, L-, S-, Ku1-band, VV, 20° i.a.)

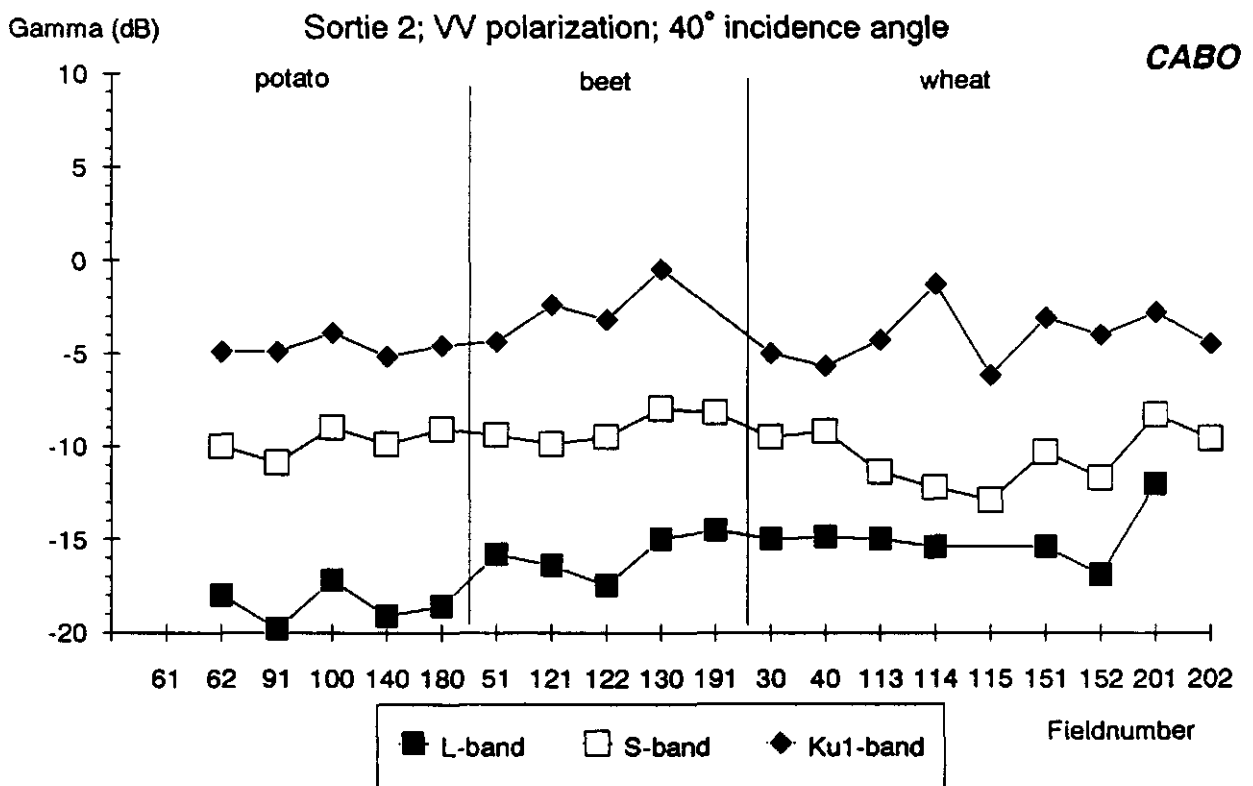


Fig. 38 Radar backscatter of the main croptypes (sortie 2, L-, S-, Ku1-band, VV, 40° i.a.)

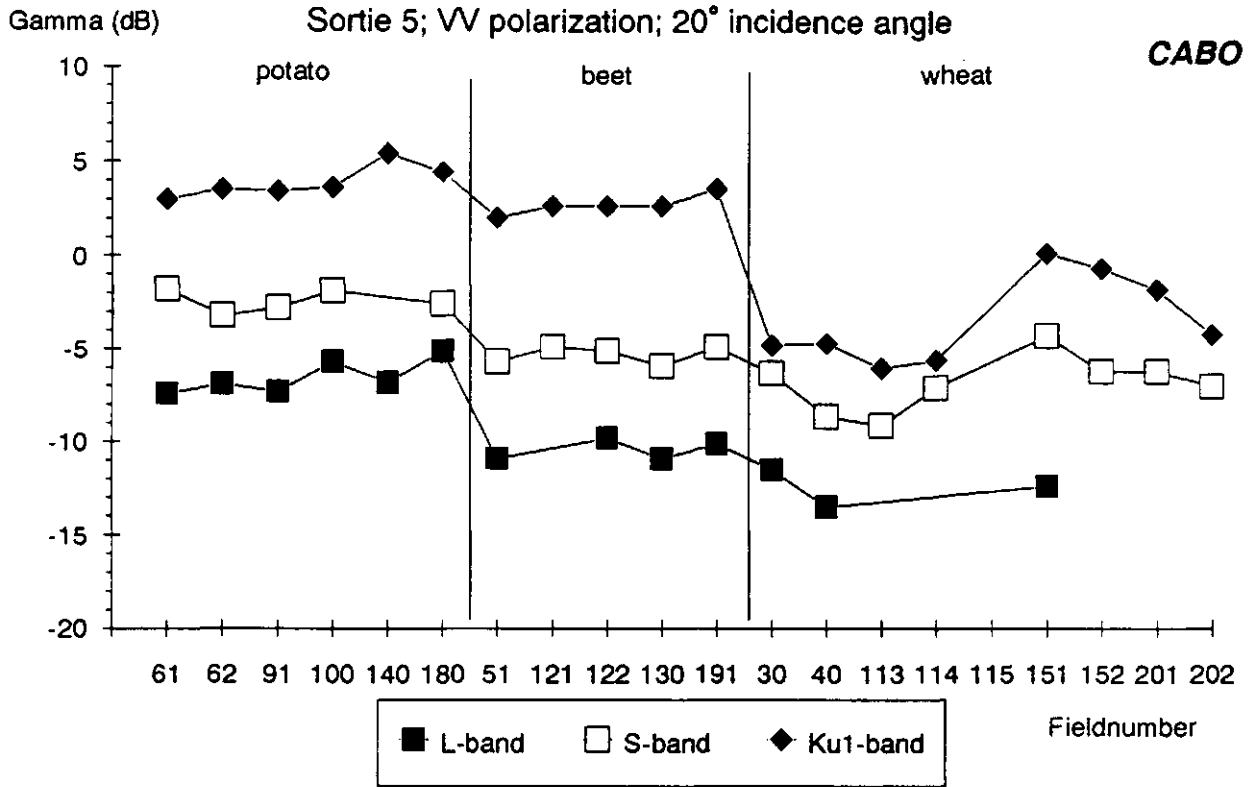


Fig. 39 Radar backscatter of the main croptypes (sortie 5, L-, S-, Ku1-band, VV, 20° i.a.)

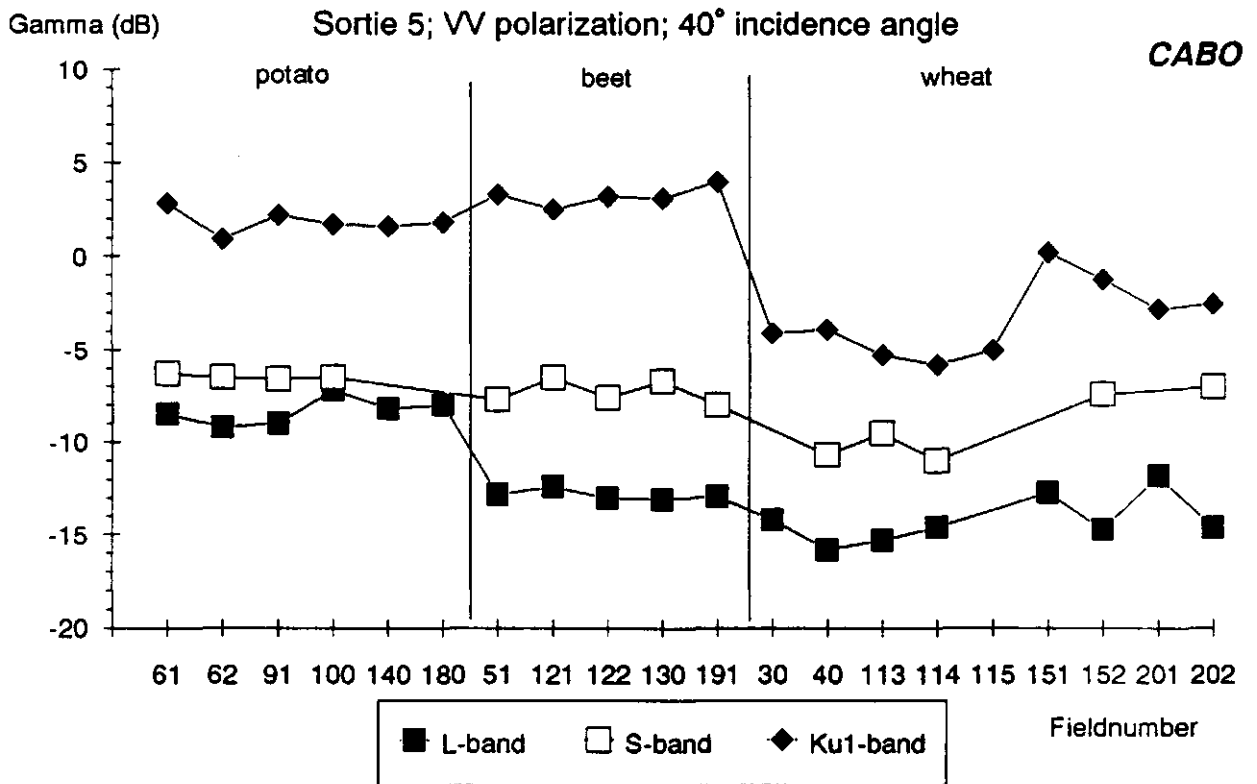


Fig. 40 Radar backscatter of the main croptypes (sortie 5, L-, S-, Ku1-band, VV, 40° i.a.)

4 Summary and conclusions

Based on the general quality analysis, the data set of the DUTSCAT 87 is rigorously reduced. The whole C- and Ku2-band, all the measurements at 70° incidence angle and all field averages with standard deviations > 3 dB are removed. The X-band was not calibrated and it will therefore only be used as a reference band (no temporal analyses; no analyses on absolute value). This reduced data set appears after a first visual interpretation fairly consistent:

- The relative position of the frequency bands is in accordance with general theory: backscatter Ku1 band > backscatter S-band > backscatter L-band.
- The field-average γ values of the different crop types are very well clustered in all frequency bands, angles of incidence and at all sorties. The relative broad cluster of wheat matches the relative large spread in the groundtruth.
- For each crop type the angular dependency of the radar backscatter is smooth in all frequency bands. For mainly bare soil, the backscatter decreases a little with increasing incidence angle while for crops (midst of the growing season) the curves are more or less horizontal.
- Crops and fields of mainly bare soil are differentiated in the different frequency bands. For mainly bare soil, the combination of the L- and the Ku1-band offers the best possibilities for discrimination. The L-band separates 'potato-soil' from 'beet-' and 'wheat-soil' (70% crop cover), and the Ku2-band separates 'beet-soil' from 'potato-' and 'wheat-soil' (70% crop cover). For crops, the most important band is the L-band, and the best combination is with the S-band. In all three bands, wheat is very well separated from beet and potato, but only in the L-band (and to some extent in the S-band) potato is separated from beet. In general, the trends between the crops are similar in the three frequency bands.
- The temporal curves of the radar backscatter of the crops are comparable in trend in all three frequency bands. For beet and potato, the backscatter increases with crop growth until the midst of the growing season (sortie 4). For wheat, the temporal curves are more or less concave: the backscatter decreases with increasing LAI until sortie 3, and then increases with decreasing LAI until harvest. However, for wheat, this pattern might equally well be caused by a relation with the soil moisture content. For all crops, the temporal trends are comparable to the trends found in the X- and Q-band in the ground based ROVE data set. In general, the range in backscatter with the growth of the crop is not very large, i.e. in the order of 4-6 dB for all three frequency bands and for all three crops (40° incidence angle). An exception is the L-band for potato in which the range is some 10 dB.
- There seems to be no correlation between the temporal backscatter of beet and potato (throughout the growing season) and the average soil moisture content (0-5 cm top soil). Even for the relatively long wavelengths in the L-band, the canopy appears opaque. A correlation between the soil moisture content and the radar backscatter appears only present for wheat. The peaks and dips in the moisture content are reproduced in the backscatter curves (especially in the L- and Ku1-band).
- The dynamics in the S-band are relatively smallest. Both the variation between the crops and the temporal variation per crop type is relatively low.

References

Attema, E., 1989, Radar signature measurements during the Agriscatt campaign, Proceedings of IGARSS'88 Symposium, Edinburgh, Scotland, 13-16 September, ESA SP-284: 1141-1144.

Bouman, B.A.M., 1987. Radar backscatter from three agricultural crops: beet, potatoes and peas. CABO report 71.

Bouman, B.A.M. and H.W.J. van Kasteren, 1989. Ground based radar backscatter measurements of wheat, barley and oats, 1975-1981. CABO report 119.

Hoekman, D.H., 1990, The Agriscatt Campaign. Radar data acquisition at agricultural countries during the 1987 and 1988 growing seasons, Agricultural University of Wageningen reports, LUW-LMK 199002.

James, G., 1989, Agriscatt 1987, Quality assessment of DUTSCAT data, ESA/EARTHNET, November 1989, Frascati.

Luik, P.C., 1990, Werkwijze voor het corrigeren van fouten in de DUTSCAT data 1987/1988, BCRS report 90-14, Delft, The Netherlands (In Dutch).

Snoeij, P. and P.J.F. Swart, 1987, The DUT airborne scatterometer, International Journal of Remote Sensing, vol. 8, no. 11, pp: 1709-1716.

Snoeij, P. and P.J.F. Swart, 1989. The Agriscatt-87 campaign. Processing of the DUTSCAT data, Final report. Telecommunication and Remote Sensing technology, Technical University Delft.

Stolp, J. et al., 1988. Agriscatt 87 Ground data collection Flevoland (NL). STIBOKA report 2027, CABO report 80.